CIRANO
Knowledge into action

NIGHTTIME LIGHT POLLUTION AND ECONOMIC ACTIVITIES: A SPATIO-TEMPORAL MODEL WITH COMMON FACTORS FOR US COUNTIES

GEORGES **BRESSON**
JEAN-MICHEL **ETIENNE**
GUY **LACROIX**

2023s-18
WORKING PAPER

CS

CIRANO
Knowledge into action

Center for Interuniversity Research and Analysis on Organizations

The purpose of the **Working Papers** is to disseminate the results of research conducted by CIRANO research members in order to solicit exchanges and comments. These reports are written in the style of scientific publications. The ideas and opinions expressed in these documents are solely those of the authors.

Les cahiers de la série scientifique visent à rendre accessibles les résultats des recherches effectuées par des chercheurs membres du CIRANO afin de susciter échanges et commentaires. Ces cahiers sont rédigés dans le style des publications scientifiques et n'engagent que leurs auteurs.

CIRANO is a private non-profit organization incorporated under the Quebec Companies Act. Its infrastructure and research activities are funded through fees paid by member organizations, an infrastructure grant from the government of Quebec, and grants and research mandates obtained by its research teams.

Le CIRANO est un organisme sans but lucratif constitué en vertu de la Loi des compagnies du Québec. Le financement de son infrastructure et de ses activités de recherche provient des cotisations de ses organisations-membres, d'une subvention d'infrastructure du gouvernement du Québec, de même que des subventions et mandats obtenus par ses équipes de recherche.

CIRANO Partners – *Les partenaires du CIRANO*

Corporate Partners – *Partenaires corporatifs*
Autorité des marchés financiers
Bank of Canada
Bell Canada
BMO Financial Group
Business Development Bank of Canada
Caisse de dépôt et placement du Québec
Desjardins Group
Énergir
Hydro-Québec
Innovation, Science and Economic Development Canada
Intact Financial Corporation
Manulife Canada
Ministère de l'Économie, de l'Innovation et de l'Énergie
Ministère des finances du Québec
National Bank of Canada
Power Corporation of Canada
PSP Investments
Rio Tinto
Ville de Montréal

Academic Partners – *Partenaires universitaires*
Concordia University
École de technologie supérieure
École nationale d'administration publique
HEC Montréal
McGill University
National Institute for Scientific Research
Polytechnique Montréal
Université de Montréal
Université de Sherbrooke
Université du Québec
Université du Québec à Montréal
Université Laval

CIRANO collaborates with many centers and university research chairs; list available on its website. *Le CIRANO collabore avec de nombreux centres et chaires de recherche universitaires dont on peut consulter la liste sur son site web.*

ISSN 2292-0838 (online version)

Nighttime light pollution and economic activities: A spatio-temporal model with common factors for US counties

Georges Bresson[*], *Jean-Michel Etienne*[†], *Guy Lacroix*[‡]

Abstract/Résumé

Excessive nighttime light is known to have detrimental effects on health and on the environment (fauna and flora). The paper investigates the link between nighttime light pollution and economic growth, air pollution, and urban density. We propose a county model of consumption which accounts for spatial interactions. The model naturally leads to a dynamic general nesting spatial model with unknown common factors. The model is estimated with data for 3071 continental US counties from 2012–2019 using a quasi-maximum likelihood estimator. Short run and long run county marginal effects emphasize the importance of spillover effects on radiance levels. Counties with high levels of radiance are less sensitive to additional growth than low-level counties. This has implications for policies that have been proposed to curtail nighttime light pollution.

L'éclairage nocturne de forte intensité est connu pour avoir des effets néfastes sur la santé et sur l'environnement (faune et flore). Cet article étudie le lien entre la pollution lumineuse nocturne et la croissance économique, la pollution de l'air et la densité urbaine. Nous proposons un modèle de consommation au niveau des comtés américains qui tient compte des interactions spatiales. Le modèle conduit naturellement à un modèle spatial dynamique général emboîté avec facteurs communs inconnus. Le modèle est estimé avec les données de 3 071 comtés continentaux américains de 2012 à 2019 à l'aide d'un estimateur de quasi-maximum de vraisemblance. Les effets marginaux des comtés à court et à long terme soulignent l'importance des effets de débordement sur la radiance locale. Les comtés caractérisés par de hauts niveaux de radiance sont moins sensibles à un accroissement de l'activité économique que ceux avec de faibles niveaux. Cela a des implications pour le design de politiques visant à réduire la pollution lumineuse nocturne.

[*] Department of Economics, Université Paris Panthéon-Assas, France georges.bresson@u-paris2.fr
[†] Department of Economics, Université Paris-Saclay, Sceaux, France jean-michel.etienne@u-psud.fr
[‡] Department of Economics, Université Laval, Québec, QC, Canada Guy.Lacroix@ecn.ulaval.ca
Corresponding author. Department of Economics, Pavillon J.-A.-DeSève, 1025, avenue des Sciences-Humaines, Université Laval, Québec (Québec) G1V 0A6, Canada.

Keywords/Mots-clés: Nighttime light pollution, air pollution, GDP, satellite data, space-time panel data model / Pollution lumineuse nocturne, pollution de l'air, PIB, données satellitaires, modèle panel spatio-temporel

JEL Codes/Codes JEL: C23, Q53

Pour citer ce document / To quote this document
Bresson, G., Etienne, J.-M. , & Lacroix, G. (2023). Nighttime light pollution and economic activities: A spatio-temporal model with common factors for US counties (2023s-18, Cahiers scientifiques, CIRANO.) https://doi.org/10.54932/SOEA8799

1. Introduction

Nighttime lighting is intimately related to economic development and growth. Satellite recordings are now widely used by social scientists and development economists as proxies for human development and wealth in subnational regions of developing countries. In developed economies, though, night light is often perceived as a nuisance. Indeed, the presence of unwanted, inappropriate or excessive artificial lighting has been coined "night-light pollution". Falchi et al. (2016) and Kyba et al. (2017) have estimated that 83% of the world's population is affected by nighttime lighting and that as much as 23% of the earth's terrestrial surface is covered by night light.

Night light pollution can take many forms: light trespass, glare, over-illumination, light clutter, sky glow, *etc.*[1] Its impact on the health and well-being of human (Sager, 2019), animal and vegetal lifeforms has become a major concern in recent years. Humans have always evolved in an environment with a clear distinction between night and day. Ubiquitous electric lighting at home and at the workplace, and the use of light-emitting electronic devices at night, have blurred this distinction (Cain et al., 2020). People now spend most waking hours surrounded by artificial lighting, reduced sunlight exposure and relatively bright nighttime lighting (Goulet et al., 2007; Martinez-Nicolas et al., 2019). Excessive nighttime light exposure can reduce circadian amplitude which has been associated with greater incidence of depressions (Jewett et al., 1994; Burns et al., 2021).

Excessive nightlight has also been shown to increase atmospheric pollution since it prevents nighttime chemical reactions that normally reduce the smog produced by the fumes emitted from cars and factories (see Stark et al., 2011; CIRES, 2011). In addition, Ściężor and Czaplicka (2020) have shown that various types of aerosols, both of natural and anthropogenic sources, exacerbates sky glow. Particulate matter (PM) related to the combustion of solid fuels in the winter as well as mists and haze are considered important light scattering sources. Anthropogenic particulate matter has the greatest impact on the brightness of the cloudless night sky glow in winter. In areas heavily polluted with light, fogs and mist are particularly important.

[1] Light trespass occurs when spill light, which is light that falls outside the area intended to be lit, is cast where it is not wanted. A typical light trespass problem occurs when a strong light enters the window of one's home from the outside. Glare is when light strikes your eyes directly from the source. Over-illumination is the excessive use of lighting, such as leaving lights on when they are not being used or using poorly designed lighting that illuminates areas that do not need to be illuminated. Light clutter refers to excessive groupings of lights, especially bright or flashing lights, which can generate confusion or accidents. Sky glow is the illumination of the night sky, most referred to as the "glow" effect that appears over populated areas at night. Sky glow is mainly a combination of reflected light from illuminated areas and badly directed light escaping into the sky, where it is scattered by the atmosphere and redirected back at the ground. If the sky glow is generally observed at distances lower than 100 km, some of them can be seen at more than 400 Km of distance. This is the case for example of the lights of Las Vegas and Phoenix in the US (Duriscoe et al., 2014).

Numerous studies have recently investigated the link between air pollution and several categories of crime. Thus Burkhardt et al. (2019) report evidence that exposure to $PM_{2.5}$ increases violent crimes at the county level while Jones (2022) finds strong evidence that dust storm activity is associated with violent crimes also at the county level in the US. Herrnstadt et al. (2021) find similar results for the City of Chicago using PM_{10} exposure. Kuo and Putra (2021) (New South Wales, Australia) and Bondy et al. (2020) (London, England) also report positive impacts of air pollution on crime. Many have also investigated the link between night light *per se* and crime. The empirical evidence brought to bear is rather ambiguous. Absence of street lighting has been found to reduce car theft and burglaries in the UK (Tompson et al., 2022) but to have opposite short-run (Chalfin et al., 2022) and long-run (Mitre-Becerril et al., 2022) effects in New-York. The latter results are based on a randomized experiment of street lighting in public housing developments. Doleac and Sanders (2015) use daily saving time (DST) to estimate the causal impact of light on criminal activity. Their results are consistent with those of Chalfin et al. (2022),Mitre-Becerril et al. (2022) and Sager (2019): The switch to DST reduces robberies during the hours with extended daylight.

The detrimental consequences of nightlight pollution has lead many to advocate eliminating or reducing it as much as possible. For example, Tucson (Arizona) has recently reduced sky glow by 7% percent after converting street lights. At least 18 states, the District of Columbia and Puerto Rico now have laws in place to reduce light pollution. The majority of states that have enacted so-called "dark skies" legislation have done so to promote energy conservation, public safety, aesthetic interests and astronomical research capabilities. Municipalities in a number of states have also been active on this issue, adopting light pollution regulations as part of their zoning. More and more cities are adopting policies to drastically reduce or even switch off public lighting during certain hours of the night (Dizon and Pranggono, 2022). Since the beginning of the war in Ukraine, faced with soaring energy prices, European cities are turning off their lights. Spain has made these measures compulsory, ordering stores to turn off their lights at night. Berlin has turned off the floodlights that illuminate 200 of its historic buildings and monuments, and a number of cities in Austria, Germany and Italy have reduced street lighting or switched off commercial signs. In France, many municipalities have taken steps to switch off street lighting completely between midnight and 5 am each night (quoted by Politico, August 3, 2022). These commitments are in line with the Green New Deal for Europe proposed by the European Commission to make the EU's climate, energy, transport and taxation policies fit for reducing net greenhouse gas emissions by at least 55% by 2030, compared to 1990 levels (European Commission, 2021).

Research suggests that light pollution is an issue primarily in industrialized countries. Gallaway et al. (2010) found that those with high rates of resource extraction typically have high levels of light pollution. Likewise, countries with high GDP and dense urban

and suburban areas also had the highest rates of light pollution. Over the past decade, and since the seminal papers of Chen and Nordhaus (2011) and Henderson et al. (2011, 2012), the links between light pollution and economic activities have been extensively investigated (see Zhao et al., 2019; Addison and Stewart, 2015, for a survey). Among the many studies, two main approaches can be distinguished: those that use satellite nighttime lights data as a proxy of GDP or to explain urban sprawl, especially for countries with poorly developed national accounting systems (see, *e.g.*, Chen and Nordhaus, 2011; Henderson et al., 2012; Addison and Stewart, 2015; Keola et al., 2015; Bickenbach et al., 2016; Chen and Nordhaus, 2019; Goldblatt et al., 2020; Gibson and Boe-Gibson, 2021; Ch et al., 2021). And those less numerous, which, on the contrary, use economic data (GDP, population,...) to model nightlight pollution (Hu and Yao, 2022).

This paper is cast within the second strand of the literature. It investigates the links between economic activities (GDP) and light pollution at the county level across the US. As per the literature, the analysis accounts for population level, urban density, air pollution, *etc.* Physical data (night light, urban density and $PM_{2.5}$) are drawn from the *Visible Infrared Imaging Radiometer Suite* (VIIRS) onboard the Suomi satellite.[2] Data on county-level GDP and population estimates are drawn from the Bureau of Economic Analysis (Aysheshim et al., 2020).[3] The purpose of the paper is to determine the short and long-run local sensitivity of light pollution to economic growth (GDP) and other conditioning variables. Policies to mitigate light pollution may indeed be more efficient in certain areas and less so elsewhere, and may also undermined by local economic growth. In order to achieve this, we extend the spatial urban models developed by Glaeser et al. (1995) and Brueckner (2003) in Section 2.[4] The manner in which we account for spatial interaction effects between the dependent and the explanatory variables leads to the so-called dynamic general nesting spatial model with common factors (Shi and Lee, 2017; Elhorst, 2021). This is detailed in Section 3. Section 4 gives the results and Section 5 concludes.

2. A spatial urban model of nighttime lights pollution and economic activities

Following Firmino Costa da Silva et al. (2017), we assume that the total output of county $i(= 1, ..., N)$ at time $t(= 1, ..., T)$ is given by a Cobb-Douglas production function:

$$Q_{it} = A_{it} L_{it}^{\beta_L} K_{it}^{\beta_K} \overline{Z}_i^{1-\beta_L-\beta_K},$$

[2]VIIRS nighttime light data have been included in the AidData geoquery tool to allow extraction at subnational levels (see Goodman et al., 2019).

[3]For population estimates, see BEA Methods Statement v2021.

[4]See also Debarsy et al. (2012) and Firmino Costa da Silva et al. (2017).

where L_{it} represents the population size of the county which proxies the number of workers, K_{it} denotes the traded capital and $\overline{Z}_i$ is fixed non-traded capital. A_{it} is the total factor productivity (TFP) which we assume depends on the TFP of other counties but whose intensity decreases with distance. More formally, let

$$A_{it} = a_{it} \prod_{j(\neq i)=1}^{N} a_{jt}^{\eta w_{ij}},$$

where the TFP A_{it} is a function of county and time-specific labor productivity and technology, a_{it}, as well as those of neighboring counties, a_{jt} $j\,(\neq i)$. The parameter η $(0 < \eta < 1)$ captures the degree of interdependence among them. Although η is assumed to be constant, the interactions between counties depends on the relative location of each, w_{ij}, which are elements of a $(N \times N)$ neighborhood matrix W_N such that $0 \leq w_{ij} \leq 1$ and $w_{ii} = 0$.

Normalizing the price of capital to one, the first-order conditions with respect to capital and labor yields the following labor demand equation:

$$s_{it} = A_{it}^{\frac{1}{1-\beta_K}} \beta_L \beta_K^{\frac{\beta_K}{1-\beta_K}} L_{it}^{\frac{\beta_L+\beta_K-1}{1-\beta_K}} \overline{Z}_i^{\frac{1-\beta_L-\beta_K}{1-\beta_K}}, \tag{1}$$

where s_{it} is the wage rate (see section A in the supplementary material).

Consumers in county i are assumed to have a Cobb-Douglas utility function for tradable goods, C_{it}, and housing, H_{it}. Following Brueckner (2003), it is further assumed that the utility level is weakly separable in both the local and distant county (dis)amenities. The latter include traffic congestion, nighttime light pollution, R_{it}, air pollution, P_{it}, *etc.* According to Glaeser et al. (1995), potential (dis)amenities can be proxied by population size since it may be argued that quality of life is inversely related to it. Formally, we generalize the Cobb-Douglas utility functions proposed by Brueckner (2003), Glaeser et al. (1995) and Firmino Costa da Silva et al. (2017) and write:

$$U_{it} = C_{it}^{1-\alpha} H_{it}^{\alpha} \left(R_{it}^{-\psi} \prod_{j(\neq i)=1}^{N} R_{jt}^{-\zeta w_{ij}} \right) \left(P_{it}^{-\kappa} \prod_{j(\neq i)=1}^{N} P_{jt}^{-\xi w_{ij}} \right) L_{it}^{-\varphi} \prod_{j(\neq i)=1}^{N} L_{jt}^{-\nu w_{ij}},$$

where $\psi > 0$, $\zeta > 0$, $\kappa > 0$, $\xi > 0$, $\varphi > 0$ and $\nu > 0$. Consumers maximize their utility subject to the following budget constraint:

$$C_{it} + p_{H_{it}} H_{it} = s_{it} L_{it}$$

by choosing C_{it} and H_{it}, where the price of the tradable good is normalized to 1 and the housing price is given by $p_{H_{it}}$. The housing demand is then given by (see section A in

the supplementary material):

$$H_{it} = \frac{\alpha s_{it} L_{it}}{p_{H_{it}}}.$$

As underlined by Firmino Costa da Silva et al. (2017), spatial equilibrium conditions insures that utility equalizes across space if labor is mobile: Higher wages are required to offset local negative attributes (pollution, crime, *etc.*). Let the common utility level at a particular point in time be denoted as V_t. In equilibrium, the indirect utility function is given by

$$V_t = \alpha^{\alpha} (1-\alpha)^{1-\alpha} s_{it} p_{H_{it}}^{-\alpha} \left(R_{it}^{-\psi} \prod_{j(\neq i)=1}^{N} R_{jt}^{-\zeta w_{ij}} \right) \left(P_{it}^{-\kappa} \prod_{j(\neq i)=1}^{N} P_{jt}^{-\xi w_{ij}} \right) L_{it}^{1-\varphi} \prod_{j(\neq i)=1}^{N} L_{jt}^{-\nu w_{ij}} \tag{2}$$

Following Firmino Costa da Silva et al. (2017) and Glaeser and Gottlieb (2009), housing floor space is produced competitively either by land (l) or by height (h). If the supply of land at a particular location is fixed, or becomes available only gradually, the prices of land (p_l) and housing (p_H) are endogenous, and thus the cost of producing hl units of structure on top of l units of land is given by $c_0 h^{\delta} l$, where $\delta > 1$. If developer maximizes profits, the housing supply is given by (see section A in the supplementary material):

$$hl = \left(p_{H_{it}} / \delta c_0\right)^{\frac{1}{\delta - 1}} l$$

Housing prices equation is achieved by the housing market equilibrium (see section A in the supplementary material):

$$p_{H_{it}} = \left(\frac{\alpha s_{it} L_{it}}{l} \right)^{\frac{\delta - 1}{\delta}} (\delta c_0)^{\frac{1}{\delta}} \tag{3}$$

Solving the system formed by labor demand (1), indirect utility (2) and housing prices (3) for the (dis)amenities R_{it} yields:

$$\log R_{it} = \frac{1}{\psi} \left[\begin{array}{l} \left\{ \frac{\delta(1-\alpha)+\alpha}{\delta(1-\beta_K)} \right\} \log A_{it} + \Theta \log L_{it} - \sum_{j(\neq i)=1}^{N} \nu w_{ij} \log L_{jt} - \sum_{j(\neq i)=1}^{N} \zeta w_{ij} \log R_{jt} \\ -\kappa \log P_{it} - \sum_{j(\neq i)=1}^{N} \xi w_{ij} \log P_{jt} + \Phi_{it} \end{array} \right]$$

Φ_{it} is a rather cumbersome function of individual specific effects through $\log \overline{Z}_i$ and time effects through $\log V_t$ (Θ and Φ_{it} are detailed in section A in the supplementary material).

Since

$$\begin{aligned}\log A_{it} &= (1-\beta_K)\log Q_{it} - \beta_L \log L_{it} + (\beta_K - 1)\,\eta \sum_{j(\neq i)=1}^{N} w_{ij}\log Q_{jt} \\ &\quad + \beta_L \eta \sum_{j(\neq i)=1}^{N} w_{ij}\log L_{jt} + D_{it}\end{aligned}$$

D_{it} is a rather cumbersome function of individual specific effects through $\log \overline{Z}_i$, $\sum_{j(\neq i)=1}^{N} \log \overline{Z}_j$ and time effects through $\sum_{j(\neq i)=1}^{N} \log a_{jt}$ (see section A in the supplementary material). We can write

$$\log R_{it} = \frac{1}{\psi}\left[\begin{array}{l} \left\{\frac{\delta(1-\alpha)+\alpha}{\delta(1-\beta_K)}\right\}(1-\beta_K)\log Q_{it} + \left\{\frac{\delta(1-\alpha)+\alpha}{\delta(1-\beta_K)}\right\}(\beta_K-1)\,\eta \sum_{j(\neq i)=1}^{N} w_{ij}\log Q_{jt} \\ + \left(\Theta - \beta_L\left\{\frac{\delta(1-\alpha)+\alpha}{\delta(1-\beta_K)}\right\}\right)\log L_{it} + \left(\beta_L\left\{\frac{\delta(1-\alpha)+\alpha}{\delta(1-\beta_K)}\right\} - \nu\right)\sum_{j(\neq i)=1}^{N} w_{ij}\log L_{jt} \\ - \sum_{j(\neq i)=1}^{N} \zeta w_{ij}\log R_{jt} - \kappa \log P_{it} - \sum_{j(\neq i)=1}^{N} \xi w_{ij}\log P_{jt} + \Phi_{it} + D_{it}\left\{\frac{\delta(1-\alpha)+\alpha}{\delta(1-\beta_K)}\right\} \end{array}\right]$$

Pooling the N individuals for one time period (*i.e.*, dual pooling), we get

$$\begin{aligned}\left(I_N + \frac{\zeta}{\psi}W_N\right)\log R_t &= \left(\frac{\left\{\frac{\delta(1-\alpha)+\alpha}{\delta(1-\beta_K)}\right\}(1-\beta_K)}{\psi} I_N + \frac{\left\{\frac{\delta(1-\alpha)+\alpha}{\delta(1-\beta_K)}\right\}(\beta_K-1)\,\eta}{\psi} W_N\right)\log Q_t + \\ &\quad \left(\frac{\Theta - \beta_L\left\{\frac{\delta(1-\alpha)+\alpha}{\delta(1-\beta_K)}\right\}}{\psi} I_N + \frac{\beta_L\left\{\frac{\delta(1-\alpha)+\alpha}{\delta(1-\beta_K)}\right\} - \nu}{\psi} W_N\right)\log L_t - \\ &\quad \left(\frac{\kappa}{\psi} I_N + \frac{\xi}{\psi} W_N\right)\log P_t + \Phi_t + D_t\left\{\frac{\delta(1-\alpha)+\alpha}{\delta(1-\beta_K)}\right\} \qquad (4)\end{aligned}$$

where $\log R_t$, $\log Q_t$, $\log L_t$ and $\log P_t$ are $(N \times 1)$ vectors, I_N is an $(N \times N)$ identity matrix and W_N is the $(N \times N)$ spatial weight matrix. Φ_t is the $(N \times 1)$ vector of Φ_{it} and D_t is the $(N \times 1)$ vector of D_{it}. Equation (4) gives the static desired level of the (log) nighttime lights pollution of the own economy (i) and of its neighbors (j) linked to explanatory variables and can be simply written as

$$Y_t^* = X_t a + W_N X_t b + \mu_t$$

where $Y_t = \left(I_N + \frac{\zeta}{\psi}W_N\right)\log R_t$, $X_t = [\log Q_t, \log L_t, \log P_t]$, and $W_N X_t = [W_N \log Q_t, W_N \log L_t, W_N \log P_t]$. Furthermore, $\mu_t\,(= \Phi_t + D_t\,(\delta\,(1-\alpha)+\alpha)\,/\,(\delta\,(1-\beta_K)))$ defines individual and time specific effects through functions of $\log \overline{Z}_i$, $\sum_{j(\neq i)=1}^{N} \log \overline{Z}_j$ and time

effects through $\log V_t$ and $\sum_{j(\neq i)=1}^{N} \log a_{jt}$. The vectors of parameters are given by

$$a = \left(\frac{\left\{ \frac{\delta(1-\alpha)+\alpha}{\delta(1-\beta_K)} \right\}(1-\beta_K)}{\psi}, \frac{\Theta - \beta_L \left\{ \frac{\delta(1-\alpha)+\alpha}{\delta(1-\beta_K)} \right\}}{\psi}, -\frac{\kappa}{\psi} \right)'$$

$$\text{and } b = \left(\frac{\left\{ \frac{\delta(1-\alpha)+\alpha}{\delta(1-\beta_K)} \right\}(\beta_K - 1)\eta}{\psi}, \frac{\beta_L \left\{ \frac{\delta(1-\alpha)+\alpha}{\delta(1-\beta_K)} \right\} - \nu}{\psi}, -\frac{\xi}{\psi} \right)'$$

Over time, counties face adjustment costs due to growth in population, economic activities, and related (dis)amenities. Thus, as in the literature on factor demands, one can assume a partial adjustment process. Whether expectations are adaptive or rational, a dynamic process of the following form is assumed (see *e.g.* Kennan, 1979; Hendry et al., 1984; Bresson et al., 1996; Blundell et al., 1996):

$$Y_t - Y_{t-1} = (1-\phi)(Y_t^* - Y_{t-1}) + u_t$$

where $0 < \phi < 1$ and u_t is a $(N \times 1)$ vector of idiosyncratic shocks, leading to

$$\begin{aligned} \log R_t =& \lambda W_N \log R_t + \phi \log R_{t-1} + \rho W_N \log R_{t-1} + \beta_1 \log Q_t + \theta_1 W_N \log Q_t + \\ & \beta_2 \log L_t + \theta_2 W_N \log L_t + \beta_3 \log P_t + \theta_3 W_N \log P_t + \phi\mu_t + u_t \end{aligned} \tag{5}$$

with

$$\lambda = -\frac{\zeta}{\psi},\ \rho = \frac{\phi\zeta}{\psi},\ \beta_1 = (1-\phi)\frac{\left\{ \frac{\delta(1-\alpha)+\alpha}{\delta(1-\beta_K)} \right\}(1-\beta_K)}{\psi},\ \beta_2 = (1-\phi)\frac{\Theta - \beta_L \left\{ \frac{\delta(1-\alpha)+\alpha}{\delta(1-\beta_K)} \right\}}{\psi},$$

$$\beta_3 = -(1-\phi)\frac{\kappa}{\psi},\ \theta_1 = (1-\phi)\frac{\left\{ \frac{\delta(1-\alpha)+\alpha}{\delta(1-\beta_K)} \right\}(\beta_K - 1)\eta}{\psi},\ \theta_2 = (1-\phi)\frac{\beta_L \left\{ \frac{\delta(1-\alpha)+\alpha}{\delta(1-\beta_K)} \right\} - \nu}{\psi},$$

$$\theta_3 = -(1-\phi)\frac{\xi}{\psi}$$

The parameter $\phi\mu_t$ in (5) captures both the individual and time specific effects. To take into account the fact that they are intertwined, we incorporate common the correlated effects Γf_t, where f_t is a $(m \times 1)$ vector of m unknown common factors and Γ is a $(N \times m)$ matrix of factor loadings. We further assume that the *i.i.d* idiosyncratic error u_t, with components $\varepsilon_t \sim (0, \sigma^2 I_N)$, possesses a spatial structure $\widetilde{W}_N$, which may or may

not be the same as W_N:

$$\begin{aligned} \log R_t &= \lambda W_N \log R_t + \phi \log R_{t-1} + \rho W_N \log R_{t-1} + \beta_1 \log Q_t + \theta_1 W_N \log Q_t \\ &\quad + \beta_2 \log L_t + \theta_2 W_N \log L_t + \beta_3 \log P_t + \theta_3 W_N \log P_t + \Gamma f_t + u_t \\ \text{with } u_t &= \tau \widetilde{W}_N u_t + \varepsilon_t \end{aligned} \tag{6}$$

In the spatial econometrics literature, such a specification is known as a dynamic general nesting spatial model with common factors (Shi and Lee, 2017; Elhorst, 2021).

In the empirical analysis, R_{it} corresponds to the monthly average nigthtime lights per square km of county i for year t, expressed in watt per square kilometer steradian, Q_{it} is be the GDP, expressed in millions of chained 2012 dollar per square km, L_{it} is the population density (population per square km) or the urban density (urban area of the county divided by the county area) and P_{it} is be the mean particulate matter ($PM_{2.5}$) concentration expressed in microgram per cubic meter ($\mu g/m^3$).

3. Data and empirical strategy

3.1. Data and prima facie evidence

The analysis is based upon data drawn from two different sources. The physical data (nighttime light, $PM_{2.5}$ and urban density) were extracted from the from *AidData geoquery tool* (Goodman et al., 2019).[5] Data on county-level GDP, population, *etc.* were provided by the Bureau of Economic Analysis (BEA) using its *Data Retrieval Application Programming Interface (API)*.[6,7] The two datasets were merged using FIPS codes (Federal Information Processing System) and cover all $N = 3071$ continental U.S. counties for the 2012–2019 period.

Nighttime lighting corresponds to the average monthly radiance (or energy luminance) measured in watt per square kilometer steradian ($Watt/km^2/sr$. See Elvidge et al., 2017, 2021).[8] Satellite readings are provided several times a day. They are usually filtered to obtain images such as the one in Figure 1, which depicts detailed point estimates of light pollution.[9] These data are then processed to obtain the average monthly radiance per county and included in the AidData geoquery tool.

Put Figure 1 here.

[5] https://www.aiddata.org/geoquery

[6] BEA Data Retrieval Application Programming Interface (API).

[7] See the appendix for a detailed description of all variables.

[8] The steradian (sr) is a unit derived from the meter (m). Its expression, in base units, is $sr = m^2 \cdot m^{-2}$. It is thus a dimensionless unit. The energy intensity is expressed in watt per steradian and the radiance, in watt per square meter steradian. The original data in the AidData geoquery tool was measured in $nanoWatt/cm^2/sr$ which we converted into $Watt/km^2/sr$.

[9] See https://www.nasa.gov/mission_pages/NPP/news/earth-at-night.html for details.

The top panel of Figure 2 shows the county-wise distribution of average monthly nighttime lights, R, for the year 2012. Not surprisingly, most densely populated cities/counties have high levels of radiance.[10] Yet, close inspection of the data reveals that a number of small counties are also plagued by intensive nighttime lighting.[11] The bottom panel of the figure depicts the average *variation* in monthly radiance between 2012 and 2019. Over that period, the average US-wide annual growth rate was 2.28%. This has translated into increased radiance in most counties, but not all. Furthermore, the intensification is far from being uniform across counties. To gain some insight into the relation between nighttime lighting, R, and GDP, Figure 3 plots state-level means over the entire 2012–2019 period. The relationship between the two appears to be log-linear.[12] As per Figure 2, there is considerable heterogeneity across states. In particular, the District of Columbia (Washington DC) has a radiance level (785.695 $Watt/km^2/sr$) that is 49 times higher than the national mean level and a GDP per square km that is 104 time higher than the national average. Likewise, while the states of New York, New Jersey, Massachusetts and Maryland have both high levels of radiance and GDP per sq. km, at the other extreme, the states of Montana, Wyoming, North & South Dakota, and Idaho have low values for both.

Put Figures 2 and 3 here.

As argued above, the heterogeneity in nighttime light exposure is very likely related to the cross-county variations in GDP as well as other factors. Table 1 reports the descriptive statistics of the main variables included in the econometric model. All variables exhibit wide variations, even when normalized by county surface. Thus, GDP (in 10^6's of chained 2012\$/km^2), Q, population density/km^2, L, urban rates (urban area/county area in percent) and air pollution ($PM_{2.5}$ concentration in microgram/meter^3), P, vary considerably across counties.

Put Table 1 about here.

As is customary with panel data, we have computed a series of CIPS unit root tests on the dependent variable as well as all exogenous variables (see Table B1 in the supplementary material).[13] The null assumption of unit roots can not be rejected for log-R

[10]This includes the Northeast region between Washington and Boston, coastal Florida, the regions of Chicago, San Francisco, Los Angeles, but also Las Vegas, Phoenix, Houston, Dallas, Denver, Seattle, Salt Lake City, ...

[11]For example, the counties of McKenzie, Mountrail, and Williams in North Dakota, the county of Bernalillo in New Mexico, the counties of Modland, Ector, Winkler in Texas and the counties of Ada, Canyon in Idaho, *etc.*

[12]The same applies for population density, urban density, and air pollution (see Figures B1 to B3 in the supplementary material).

[13]Cross-sectional augmented IPS (CIPS) unit root test (Pesaran, 2007) allows for cross-sectional dependence by augmenting the Im-Pesaran-Shin (IPS) unit root test (Im et al., 2003) with a cross-

(radiance), log-Q (GDP/km^2) and urban rate. Conversely, trend stationary processes are not rejected at the 5% level for log-L (population density) and the log-P (air pollution). The effect of these unit roots is likely to be neutralized by the incorporation of common correlated factors in the econometric specification. Additional unit root tests will be conducted on the estimated residuals to validate this.

For estimation purposes, we computed a spatial matrix based on Haversine distances (in km) between county centroids using their latitudes and longitudes.[14] The distances range between 6.23 km and 3686.92 km, with an average of 1366.36 km. These are unreasonably large (quartiles $Q_1 = 766.96$ km and $Q_3 = 1230.61$ km). Thus we have resorted to use a spatial distance matrix based on the 15 nearest neighboring counties. Doing so yields a mean distance of 73.67 km, and 10^{th} percentile = 37.22 km, $Q_1 = 48.43$ km, $Q_3 = 86.96$ km and 90^{th} percentile = 117.88 km. These are more in line with sky glow radiance which are between 6.23 km and 401.02 km (see Duriscoe et al., 2014). From this spatial matrix, we define the row-normalized Haversine inverse distance matrix (W_N) which has a non-sparsity rate of 0.488% and whose non-zero weights (w_{ij}) range between 0.0229 and 0.3283 with an average of 0.0666 (see Figure B4 in the supplementary material).

3.2. The econometric methodology

The model we specify belongs to the class of dynamic general nesting spatial models with common factors and can be estimated using the quasi maximum likelihood (QML) estimation method of Shi and Lee (2017). Indeed, the specification in equation (6) is of the form:

$$\begin{aligned} Y_t &= \lambda W_N Y_t + \phi Y_{t-1} + \rho W_N Y_{t-1} + X_t\beta + \Gamma f_t + u_t \\ &\quad \text{with } u_t = \tau \widetilde{W}_N u_t + \varepsilon_t \end{aligned} \tag{7}$$

where Y_t is an N-dimensional column vector of observed dependent variables and X_t is an $(N \times (K-2))$ matrix of exogenous regressors, so that the total number of right-hand

section average. The IPS and CIPS tests relax the assumption of a common autoregressive parameter in the augmented Dickey-Fuller (ADF) specification contrary to other standard tests such as the Levin-Lin-Chu, Harris-Tzavalis or Breitung tests.

[14]The county distances are great-circle distances calculated using the Haversine formula based on internal points in the geographic area. The Haversine formula is given by

$$d = 2r \arcsin\left(\sqrt{\sin^2\left(\frac{\Phi_2 - \Phi_1}{2}\right) + \cos\Phi_1 \cos\Phi_2 \sin^2\left(\frac{\Lambda_2 - \Lambda_1}{2}\right)}\right).$$

d is the distance between the two points along a great circle of the sphere (Earth). It is the spherical distance (*i.e.*, the shortest distance between two points on the surface of a sphere). r is the radius of the sphere (637.8137 km for Earth). Φ_1 and Φ_2 are the latitudes of points 1 and 2 in radians, respectively. Likewise, Λ_1 and Λ_2 are the longitudes of points 1 and 2 in radians, respectively .

side variables is equal to K $(Y_{t-1}, W_N Y_{t-1}, X_t)$.[15] The advantage of this model is that it accommodates two types of cross sectional dependences, namely, local dependence and global (strong) dependence. Individual units are potentially impacted by time varying unknown common factors f_t, which captures global (strong) dependence. The number of unobserved factors is assumed to be a fixed constant r that is much smaller than N and T. The matrix of $(N \times r)$ factor loadings Γ and the $(T \times r)$ factors $F_T = (f_1, f_2, \cdots, f_T)'$ are not observed and are treated as parameters. The $(N \times N)$ spatial weights matrices W_N and $\widetilde{W}_N$ are used to model spatial dependences. The term $\lambda W_N Y_t$ describes the contemporaneous spatial interactions, ϕY_{t-1} captures the pure dynamic effect and $\rho W_N Y_{t-1}$ is a spatial time lag of interactions that captures diffusion. λ is the spatial dependence parameter, ϕ is the autoregressive time dependence parameter and ρ is the spatio-temporal diffusion parameter. As stated above, the idiosyncratic error u_t depends on ε_t which are assumed i.i.d.$(0, \sigma^2 I_N)$, where I_N is a $(N \times N)$ identity matrix. u_t also possesses a spatial error component structure $\widetilde{W}_N$, which may or may not be the same as W_N. The parameters of (7) are $\theta = (\delta', \lambda, \tau)'$ with $\delta = (\phi, \rho, \beta')'$, σ^2, Γ and F_T. The predetermined and the exogeneous variables are collected in a $(N \times K)$ matrix $Z_t = [Y_{t-1}, W_N Y_{t-1}, X_t]$. Denote $S(\lambda) = I_N - \lambda W_N$ and $M(\tau) = I_N - \tau \widetilde{W}_N$. The sample averaged quasi-log likelihood function is

$$\begin{aligned} \log Q_L\left(\theta, \sigma^2, \Gamma, F_T\right) &= -\frac{1}{2}\log 2\pi - \frac{1}{2}\log \sigma^2 + \frac{1}{N}\log |S(\lambda)M(\tau)| \\ &\quad -\frac{1}{2\sigma^2 NT}\sum_{t=1}^{T}\left(S(\lambda)Y_t - Z_t\delta - \Gamma f_t\right)' \\ &\quad \times M'(\tau)M(\tau)\left(S(\lambda)Y_t - Z_t\delta - \Gamma f_t\right) \end{aligned} \tag{8}$$

Concentrating out σ^2 from the objective function (8) and dropping the constant terms leads to

$$\begin{aligned} \log Q_L\left(\theta, \widetilde{\Gamma}, F_T\right) &= \frac{1}{N}\log |S(\lambda)M(\tau)| \\ &\quad -\frac{1}{2}\log \left\{ \begin{array}{l} \frac{1}{NT}\sum_{t=1}^{T}\left(M(\tau)\left(S(\lambda)Y_t - Z_t\delta\right) - \widetilde{\Gamma} f_t\right)' \\ \times \left(M(\tau)\left(S(\lambda)Y_t - Z_t\delta\right) - \widetilde{\Gamma} f_t\right) \end{array} \right\} \end{aligned}$$

[15] In our case, the $X = [x_t, W_N x_t]$ matrix contains both unspatialized (x_t) and spatialized $(W_N x_t)$ exogeneous variables where $x_t = [\log Q_t, urban\ rate_t, \log P_t]$.

where $\widetilde{\Gamma} = M(\tau)\Gamma$. Shi and Lee (2017) concentrate out the factors and their loadings using the principal component theory to get the following concentrated log-likelihood:[16]

$$\begin{aligned}\log Q_L(\theta) &= \max_{F_T,\widetilde{\Gamma}} \log Q_L\left(\theta, \widetilde{\Gamma}, F_T\right) \\ &= \frac{1}{N}\log|S(\lambda)M(\tau)| - \frac{1}{2}\log L_T(\theta)\end{aligned}$$

with

$$\log L_T(\theta) = \frac{1}{NT}\sum_{i=r+1}^{N} \varpi_i \left(\begin{array}{l} M(\tau)\left(S(\lambda)Y - \sum_{k=1}^{K} Z_k\delta_k\right) \\ \times \left(S(\lambda)Y - \sum_{k=1}^{K} Z_k\delta_k\right)' M'(\tau) \end{array} \right)$$

where Y (resp. Z_k) is the $(N \times T)$ matrix of the dependent variable (resp. of the kth explanatory variable). The estimate for $\widetilde{\Gamma}$ can be obtained as the eigenvectors associated with the first r largest eigenvalues of $M(\tau)\left(S(\lambda)Y - \sum_{k=1}^{K} Z_k\delta_k\right)\left(S(\lambda)Y - \sum_{k=1}^{K} Z_k\delta_k\right)' M'(\tau)$. By inverting N and T, the estimate for F_T can be similarly obtained.

If we interpret the factors f_t as omitted variables, an exploratory first stage regression can be used to determine how many are likely present in the data. Several approaches have been proposed to that end such as Cattell (1966)'s scree plot test, Bai and Ng (2002)'s PC and IC criteria, Onatski (2010)'s edge distribution estimator and Ahn and Horenstein (2013)'s eigenvalue ratio tests.[17]

4. Estimation results

In order to investigate the robustness of our results, we have estimated three different specifications: (1) the dynamic spatial autoregressive model (DSAR) with fixed effects, (2) the dynamic spatial Durbin model (DSDM) with fixed effects and (3) the dynamic general nesting spatial panel model with common correlated effects (DGNSP-CCE) as in equation (6).[18] Note that the DSAR and DSDM models are nested within the DGNSP-

[16] For an $(N \times T)$ matrix H_T:

$$\min_{F_T,\widetilde{\Gamma}} \operatorname{tr}\left(\left(H_T - \widetilde{\Gamma}F_T'\right)\left(H_T - \widetilde{\Gamma}F_T'\right)'\right) = \sum_{i=r+1}^{N} \varpi_i\left(H_T H_T'\right)$$

where $\varpi_i(A)$ denotes the ith largest eigenvalue of an $(N \times N)$ symmetric matrix A with eigenvalues listed in a decreasing order such that $\varpi_N(A) \leq \varpi_{N-1}(A) \leq \cdots \leq \varpi_1(A)$.

[17] See Ditzen and Reese (2023) for a recent synthesis. Shi and Lee (2017) have proposed to start by consistently estimate the regression coefficients and then to determine the number of factors from the residuals. This ensures the number is estimated consistently.

[18] The DSAR and DSDM specifications correspond to :

$$\begin{aligned} DSAR: Y_t &= \lambda W_N Y_t + \phi Y_{t-1} + \rho W_N Y_{t-1} + x_t\beta + \xi + \varepsilon_t \\ DSDM: Y_t &= \lambda W_N Y_t + \phi Y_{t-1} + \rho W_N Y_{t-1} + x_t\beta + W_N x_t\beta + \xi + \varepsilon_t \end{aligned}$$

CCE. As per the above discussion, we conducted a series of tests proposed by Cattell (1966), Onatski (2010) and Ahn and Horenstein (2013). All concluded that the data was compatible with $r = 2$ common factors (see Section C in the supplementary material).

Table 2 reports the parameter estimates of the three specifications as well as several specification tests.[19,20] As shown in the bottom panel, all three models satisfy the the stationarity condition ($\lambda + \phi + \rho < 1$) based on a $\chi^2(1)$ Wald test (see Yu et al., 2008). Likewise, the data are consistent with the assumption that the spatio-temporal diffusion parameter is equal to the negative of the product of the spatial dependence parameter and the autoregressive time dependence parameter ($\rho = -\lambda\phi$). Parent and LeSage (2011) have shown that the latter greatly simplifies the estimation of such models. This is perhaps why it is customarily imposed in empirical work. Finally, the Juodis and Reese (2022) cross-dependence test, CD_W, confirms the independence of the estimated residuals.[21] The middle panel reports the R^2 statistics as well as the estimated variance parameter, σ^2. Overall, the three specifications yield similar estimates of σ^2 and fit the data relatively well.[22]

The main differences between the models occur with respect to the slope parameters. Though the DSAR and DSDM models yield similar estimates for λ, ϕ and ρ, they differ with respect to the direct impact of pollution on radiance. Whereas the DSAR model finds no relation between the two, the DSDM model concludes the opposite. Note that the parameter is negative, which implies that additional air pollution lowers local radiance. Yet, the fact that the parameter of the spatialized air pollution ($W_N \log P$) is positive and statistically significant indicates that the spillover effects are important. Thus, the radiance level in county i increases with the $PM_{2.5}$ concentration in county j. Taken together, the two estimates suggest there is a positive link between air pollution and local radiance as found by *e.g.* Ścieżor and Czaplicka (2020). Finally, note that neither specifications find a relation between urban rate and radiance, but that both imply that

where μ is the $(N \times 1)$ vector of fixed effects (see Lee and Yu, 2015). The QML estimation methods of the DSDM and DSAR models are available in the `R` library *SDPDmod*. The Matlab code of the QML estimation method of Shi and Lee (2017) is available on Wei Shi's web page (https://sites.google.com/view/wei-shi). His Matlab code was executed within our `R` code using the *matlabr* library, an interface that allows system call to Matlab.

[19] For the sake of brevity, we do not report the estimates of the two common factors, f_t, nor of the matrix of the factor loadings, Γ.

[20] We tested different specifications in which the introduction of the variable log(population/km^2) ($\log L$) always proved irrelevant whether the urban rate was present or not.

[21] We have used the CD_W test instead of the CD test proposed by Pesaran (2004) because Juodis and Reese (2022) have shown that the CD test tends to over reject the null in the presence of latent factors. Juodis and Reese (2022) have instead proposed a randomized test statistic to correct for over-rejection (see also Pesaran and Xie, 2021).

[22] While all three specifications fit the data relatively well, the DGNSP-CCE provides yet a better fit for counties with values such as the District of Columbia: The estimated quantiles are closer to the observed quantiles and the normal Q-Q plot of residuals highlights the very good fit of the DGNSP-CCE model (see Figure D6 in the supplementary material).

spatial dependence (λ) is somewhat larger than persistence (ϕ).

The last two columns of Table 2 report the parameter estimates and the T-statistics of the DGNSP-CCE model. Contrary to the two other models, all the parameters are significantly different from zero (except for the spatialized urban rate, W_NUrban rate). While the impact of the spatial dependence ($\lambda = 0.9584$) is still sizable, the autoregressive time dependence effect has decreased significantly ($\phi = 0.3375$). As with the other specifications, the temporal dynamics is less important than the spatial dynamics, albeit both are much smaller in magnitude. The parameter estimates of GDP/km^2, $\log Q$, and of air pollution, $\log P$, are slightly larger in absolute value than their spatialized counterparts. For reasons mentioned below, these can not be directly compared. Lastly, note that the parameter estimate of τ is significantly different from zero. Thus, the DGSNP-CCE specification must be preferred to the other two. The incorporation of a spatial error component structure in the disturbances u_t as in equation (6) modifies most slope parameters as well as their statistical significance. As mentioned above, the null assumption of unit roots could not be rejected for certain covariates. When computing IPS and CIPS unit root tests on the estimated residuals, as conjectured, the null hypothesis is fortunately rejected in all three specifications (see Table D2 in the supplementary material).

Put Table 2 here.

The parameter estimates of the DGNSP-CCE model do not correspond to marginal effects (see LeSage and Pace, 2009) and so may not be directly compared to those of the DSAR or DSDM models. On the other hand, short and long run direct, indirect and total effects may be computed through impact multipliers. Thus, let $\partial \log R_{ti}/\partial x_{k,ti}$ represent the contemporaneous direct effect on county i's average monthly radiance arising from a change in its kth explanatory variable (see Debarsy et al., 2012; Elhorst, 2014). The cross-partial derivative $\partial \log R_{tj}/\partial x_{k,ti}$ measures the contemporaneous spatial spillover effect on county j, $j \neq i$, of an increase in i's kth explanatory variable. Since the model is dynamic, the partial derivatives of a change $x_{k,ti}$ may be computed for each county at various time horizons $t + s$. Written in a matrix form, and following LeSage and Pace (2009), the cumulative direct effect (*i.e.*, cumulative own-county impacts) is measured as the average of the diagonal elements, while the cumulative indirect effect (*i.e.*, diffusion over space and time) is measured by the average of the row sums of the non-diagonal elements of that matrix. Naturally, the cumulative total effect is the sum of the cumulative direct and indirect effects (see Elhorst, 2021, and the supplementary material).

Put Table 3 here.

Table 3 reports the short and long run direct, indirect and total marginal effects of various covariates on the logarithm of average monthly radiance. The direct short run

elasticities of average monthly radiance relative to GDP/km^2 range between $[0.026; 0.027]$ while spillover effects range between $[0.001; 0.095]$ leading to total short run elasticities comprised between 0.027 and 0.122 with a sample mean at 0.505. In the long run, the total elasticities increase to $[0.041; 1.54]$ with a mean at 0.069. Figure 4 reveals the spatial and temporal differences in the total marginal effects of a 1% increase in GPD/km^2. Interestingly, the maps show that counties with highest short and long run elasticities are not necessarily those the highest radiance. Thus, locations such as Los Angeles, Las Vegas, Phoenix, Miami, Chicago, New York ... are little impacted by a 1% increase in their respective GDP/km^2 (see Figure 2). It is as if their respective counties had reached such a level of light pollution that any increase in economic activity could hardly have any additional effect. On the other hand, nighttime light pollution of large peri-urban areas around large cities such as Seattle, San Francisco, Denver, ... are very sensitive to increases in GDP/km^2. Likewise, clusters of counties located on the Utah-Idaho border or the Washington-Idaho border, for example, are also highly sensitive. It is therefore in such areas that pollution control policies may yield the greatest benefits. Interestingly, a one-percentage point increase in urban rate increases radiance but by a much larger magnitude than GDP/km^2. In addition, spillover effects are way more important than own-effects, and total effects exhibit considerable heterogeneity in the long run ($[0.029; 0.998]$. See Figure 5). Finally, air pollution is found to have the greatest impact on radiance. A 1% increase in $PM_{2.5}$ translates into increases in radiance anywhere between 0.29–3.82 (short run) and 0.43–5.0 (long run) (see Figure 6). The direct effects are relatively constant and similar in the short and long run. The indirect effects, on the other hand, increase steadily as we move along the different quantiles and dominate the direct effects almost throughout.

Put Figures 4, 5 and 6 here.

5. Conclusion

Nighttime light pollution has been shown to impact health, to disturb fauna and flora, and to impact crime among other things. In this paper, we seek to quantify the link between economic growth and nighttime light pollution. To that end, we use detailed economic and physical data for 3071 counties in continental USA over the 2012-2019 period. We extend a standard spatial urban model of consumption à la Firmino Costa da Silva et al. (2017) to establish a link between the two. In particular, the model shows how light pollution (radiance) depends upon wealth (GDP), urban density and air pollution. The proposed spatial urban model additionally accounts for spatial interaction effects and leads to a dynamic general nesting spatial model with common factors. The model is estimated using a QML estimator.

According to our results, nighttime light pollution depends both upon own (direct) GDP and that of neighboring counties (spillover effects). Both the short and long run marginal effects emphasize the importance of spillover effects on radiance levels. The same applies to urban density and air pollution. Interestingly, our results unearth considerable county-wise heterogeneity in radiance response: Those with high levels of radiance are little affected by further increases in wealth. Those with lower levels are much more sensitive. It follows that policies to mitigate light pollution are likely to be more successful in the former than in the latter.

The dynamic general nesting spatial models with common correlated factors (DGNSP-CCE) nests both the Dynamic Spatial Autoregressive Model (DSAR) and the Dynamic Spatial Durbin Model (DSDM). The DGNSP-CCE outperforms the other two despite the fact that all three fit the data rather well. This is essentially due to the introduction of the common factors. Yet, the model could eventually be enriched by introducing additional covariates such as highway networks, transport flows, business centers, land cover classification (urban area, cropland, grassland, wetland, forest, *etc.*). This will be the subject of future research.

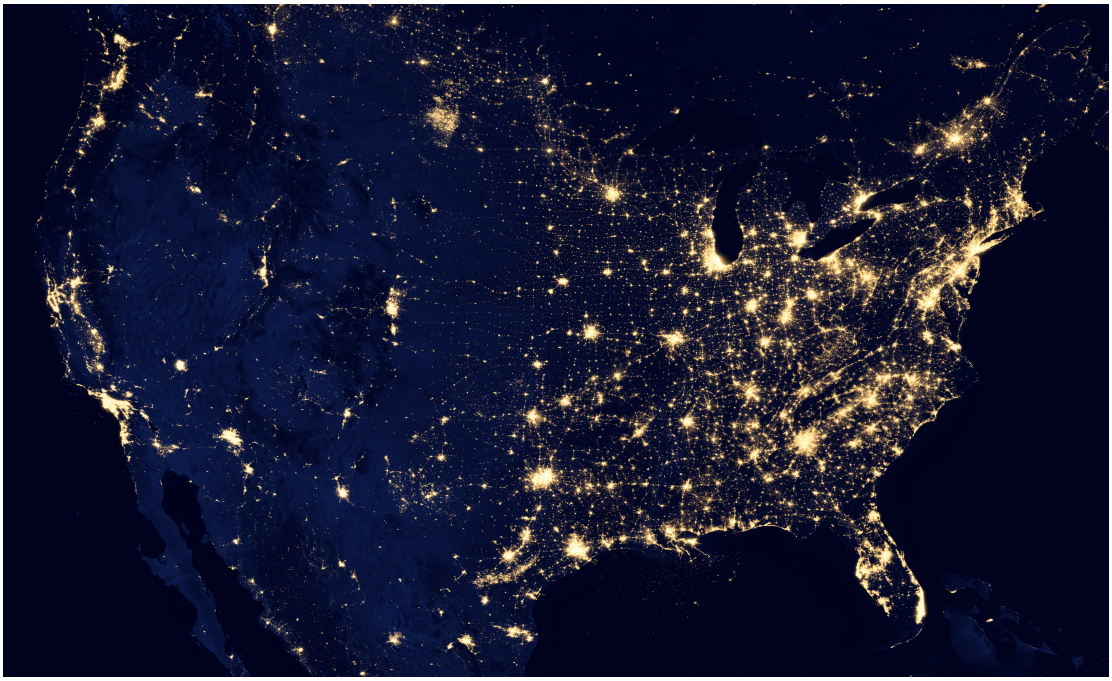

Figure 1: Continental United States at night - April-October 2012.

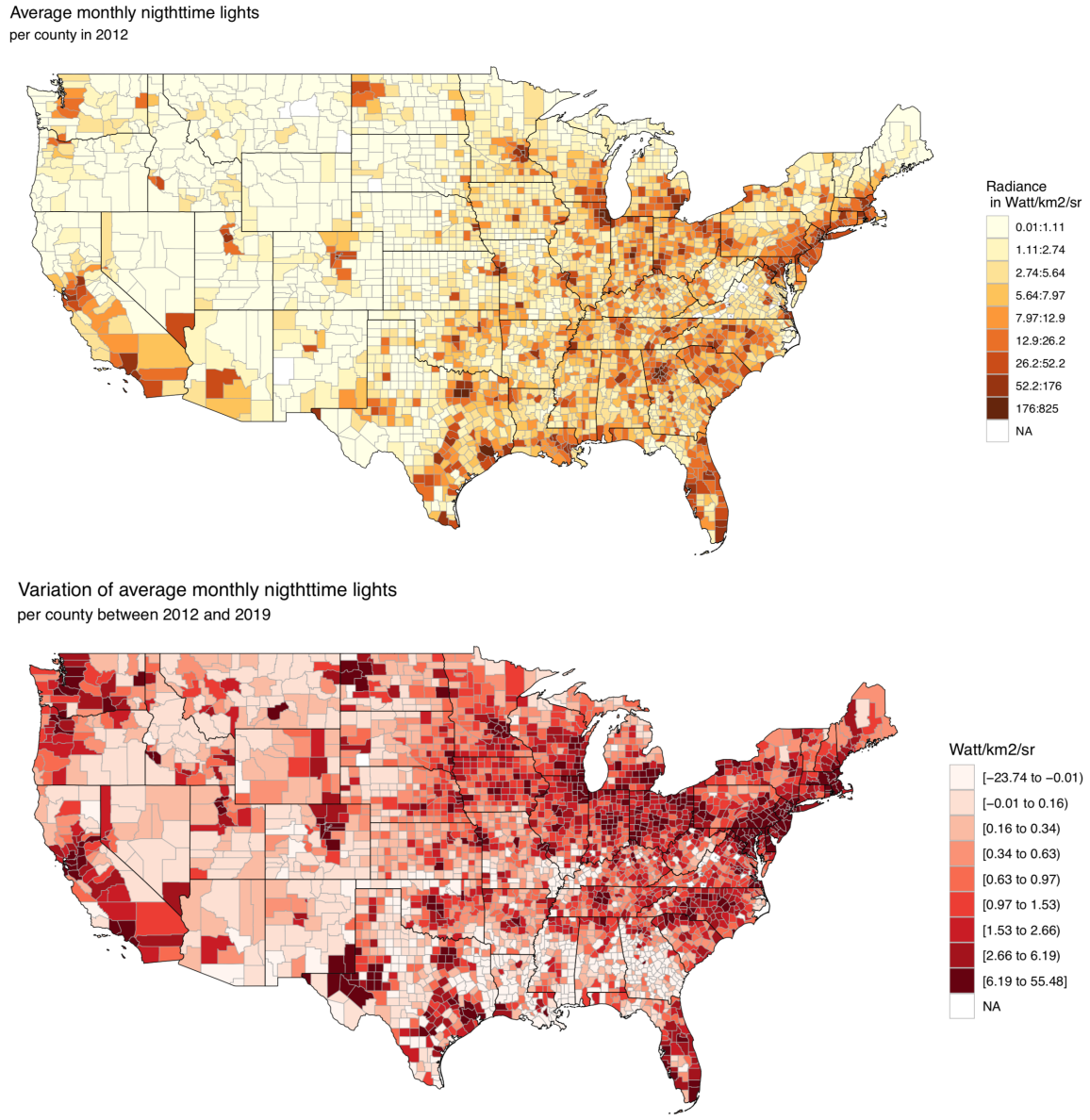

Figure 2: Average monthly nighttime lights per county in 2012 and variation between 2012 and 2019.

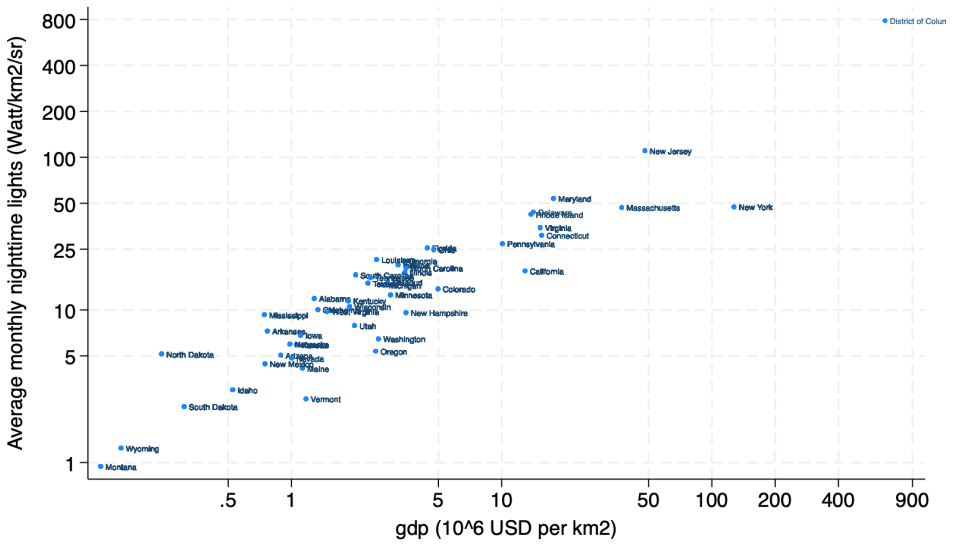

Figure 3: Scatter plot of state means of average monthly radiance and GDP/km^2.

Table 1: Descriptive statistics, $N = 3071$ US counties (2012-2019).

	Mean	Min	Max	Std.dev
Radiance	15.997	0.008	929.812	44.691
GDP	562.309	7.648	726943.301	24343.068
GDP/km^2	6.384	0.026	7282.567	123.651
Population	103.615	0.008	10094.865	330.881
Population density	80.354	0.049	18769.750	486.056
Urban rate	2.748	0.000	85.912	7.901
$PM_{2.5}$	8.916	3.333	19.501	2.139

Radiance: average monthly radiance in $Watt/km^2/sr$.
GDP: in millions of chained 2012 dollar.
GDP/km^2: in millions of chained 2012 dollar/km^2.
Population: in thousands of inhabitants.
Population density: population/km^2.
Urban rate: urban area/county area.
$PM_{2.5}$: particulate matter ($PM_{2.5}$) concentration in microgram per cubic meter ($\mu g/m^3$).

Table 2: Dynamic spatial panel models of log-average monthly radiance
$N = 3071$ US counties, $2012 - 2019$

	DSAR		DSDM		DGNSP-CCE	
	Coef.	T-stat	Coef.	T-stat	Coef.	T-stat
$\lambda : W_N \log R$	0.905	212.274	0.901	205.918	0.958	317.477
$\phi : \log R_{-1}$	0.748	120.529	0.747	119.708	0.338	47.014
$\rho : W_N \log R_{-1}$	-0.726	-97.051	-0.729	-95.530	-0.326	-42.345
Covariates:						
$\log Q$	0.033	5.304	0.033	4.657	0.026	3.320
$\log P$	0.021	1.059	-0.350	-7.812	0.236	2.311
Urban rate	0.001	0.383	-0.003	-0.911	0.008	2.029
Spatialized covariates:						
$W_N \log Q$			-0.015	-1.085	-0.024	-2.014
$W_N \log P$			0.428	8.257	-0.188	-1.763
W_N Urban rate			0.012	1.576	0.000	-0.673
Spatial error component:						
τ					-0.472	-17.256
σ^2	0.055		0.066		0.064	
R^2	0.978		0.974		0.974	
Adjusted R^2	0.978		0.974		0.964	
Tests:	Test	P-value	Test	P-value	Test	P-value
Wald: $\lambda + \phi + \rho = 1$	210.255	0.000	229.523	0.000	60.470	0.000
Wald: $\rho = -\lambda\phi$	0.000	0.999	0.000	0.999	0.906	0.341
CD_W	0.061	0.952	0.082	0.935	0.254	0.800

DSAR: Dynamic Spatial AutoRegressive model with fixed effects.
DSDM: Dynamic Spatial Durbin Model with fixed effects.
DGNSP-CCE: Dynamic General Nesting Spatial Panel model with Common Correlated Effects.
CD_W: Juodis and Reese (2022) cross-dependence test.

Table 3: Short run and long run direct, indirect and total marginal effects on average monthly radiance

		Min	10%	25%	50%	75%	90%	Max	Mean
GDP/km^2									
Short run	Direct	0.026	0.026	0.026	0.026	0.026	0.026	0.027	0.026
	Indirect	0.001	0.012	0.018	0.024	0.029	0.036	0.095	0.024
	Total	0.027	0.038	0.045	0.050	0.055	0.062	0.122	0.050
Long run	Direct	0.039	0.040	0.040	0.040	0.040	0.040	0.041	0.040
	Indirect	0.002	0.015	0.023	0.029	0.036	0.043	0.113	0.030
	Total	0.041	0.055	0.062	0.069	0.075	0.083	0.154	0.069
Urban rate									
Short run	Direct	0.009	0.010	0.010	0.011	0.011	0.012	0.019	0.011
	Indirect	0.011	0.093	0.142	0.183	0.225	0.275	0.733	0.186
	Total	0.020	0.103	0.153	0.194	0.235	0.286	0.752	0.197
Long run	Direct	0.013	0.015	0.016	0.016	0.017	0.018	0.028	0.016
	Indirect	0.015	0.130	0.196	0.251	0.305	0.372	0.970	0.254
	Total	0.029	0.145	0.212	0.267	0.322	0.390	0.998	0.271
$PM_{2.5}$ concentration									
Short run	Direct	0.238	0.244	0.246	0.248	0.250	0.253	0.289	0.249
	Indirect	0.052	0.449	0.685	0.884	1.083	1.324	3.535	0.898
	Total	0.291	0.694	0.932	1.132	1.332	1.577	3.824	1.147
Long run	Direct	0.360	0.368	0.370	0.373	0.376	0.380	0.429	0.374
	Indirect	0.073	0.612	0.926	1.185	1.441	1.755	4.576	1.200
	Total	0.432	0.982	1.297	1.558	1.816	2.138	5.005	1.574

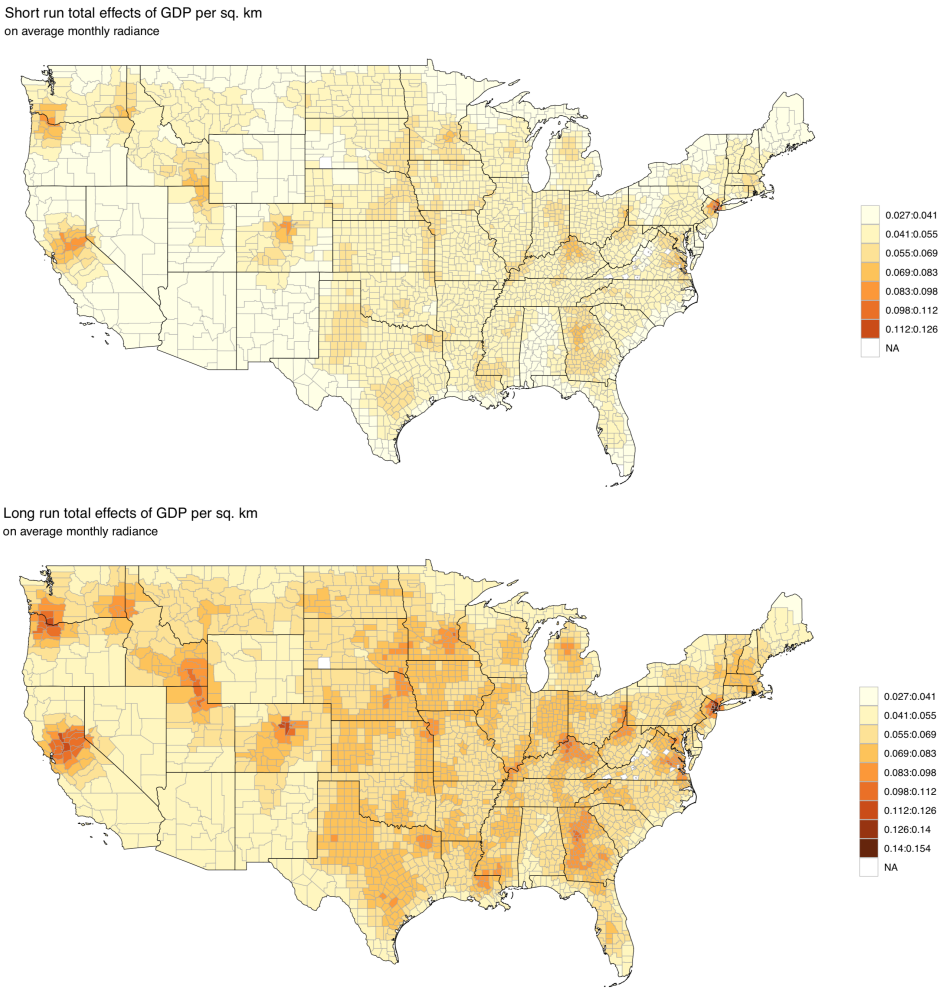

Figure 4: Short run and long run total marginal effects of GDP/km^2 on average monthly radiance.

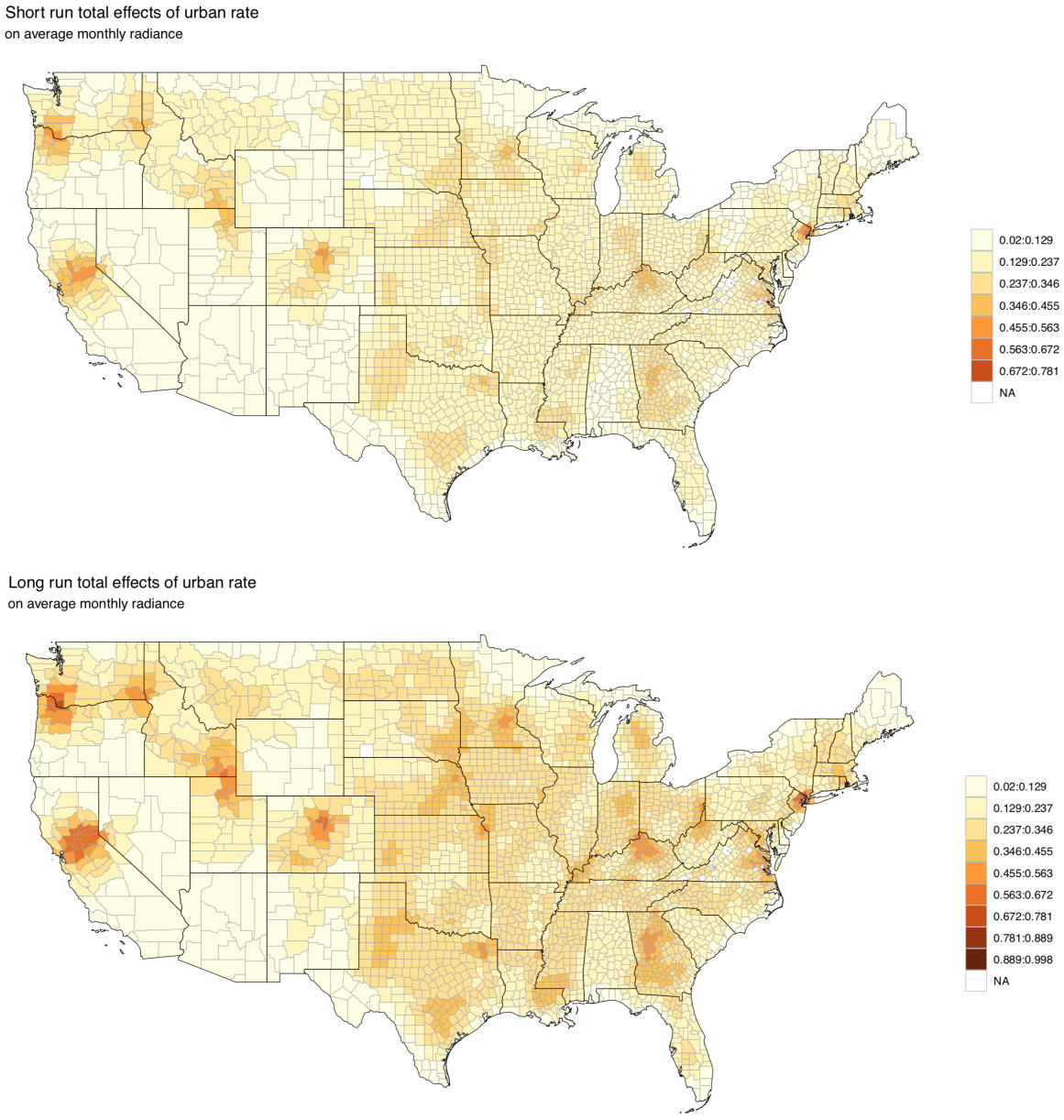

Figure 5: Short run and long run total marginal effects of urban rate on average monthly radiance.

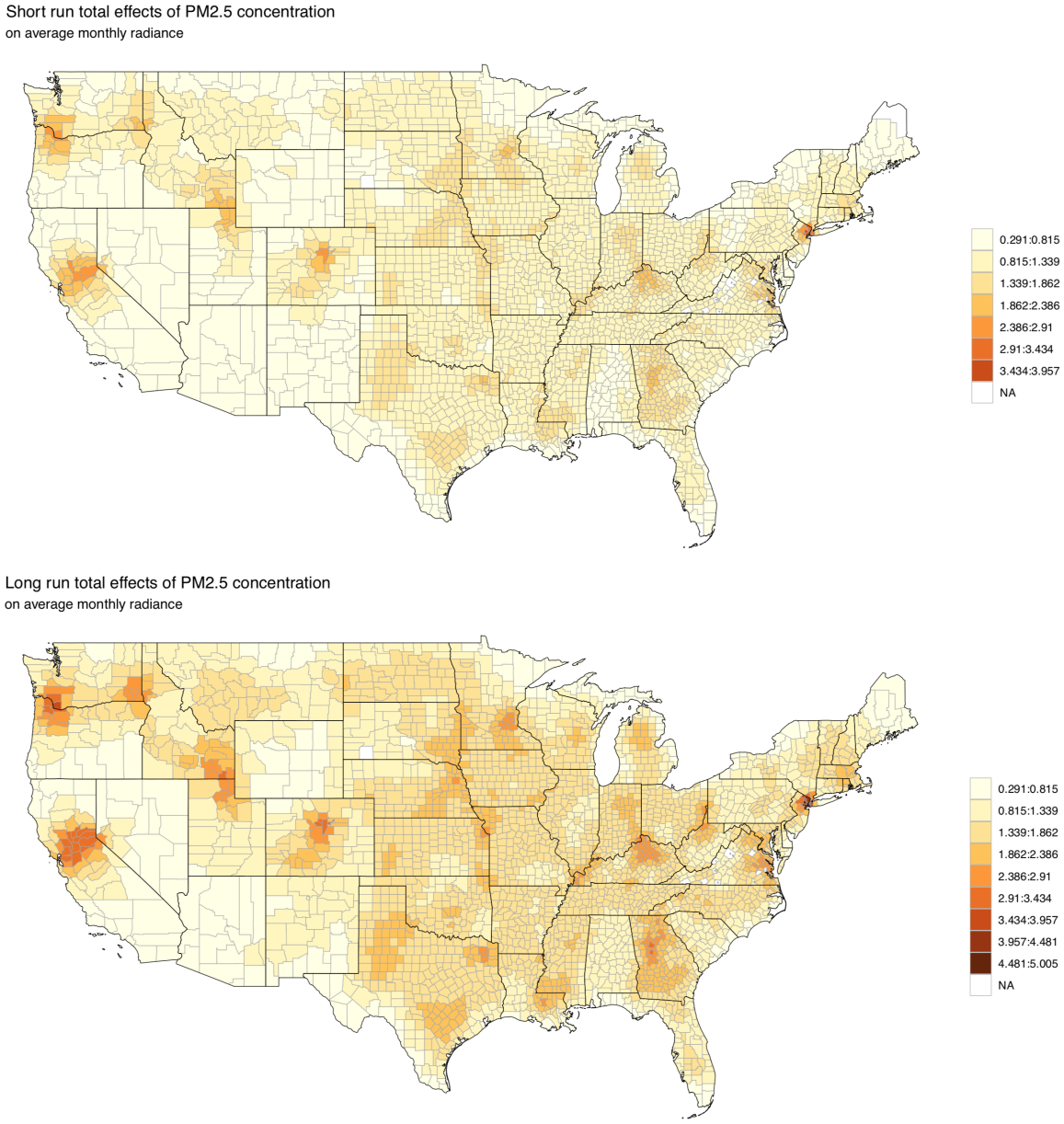

Figure 6: Short run and long run total marginal effects of $PM_{2.5}$ concentration on average monthly radiance.

A. Appendix. Data sources

A.1. Nighttime light & Air pollution

The physical data used in the paper were extracted using the AidData Geoquery tool (Goodman et al., 2019).[23] The dependent variable, nighttime light, comes from the Visible Infrared Imaging Radiometer Suite (VIIRS) Day/Night Band lights data. It corresponds to the average monthly radiance (or energy luminance) measured in watt per square kilometer steradian ($Watt/km^2/sr$) (see Elvidge et al., 2017, 2021).[24] The Federal Information Processing System (FIPS) is used to map the VIIRS data at the county level. Satellite data are provided several times a day and are filtered so as to obtain detailed point estimates of light pollution.[25] VIIRS high-resolution lighting data are updated monthly and have the potential to create a new surge in nighttime light-based studies that focus on social and economic activities. See NOAA Earth Observation Group (VIIRS Nighttime Lights).

Urban area data are drawn from European Space Agency land cover program.[26] As many as 22 land cover classes per pixel, including urban areas, are defined using the Land Cover Classification System (LCCS) developed by the United Nations Food and Agriculture Organization. The LCCS categories were grouped according to their Intergovernmental Panel on Climate Change (IPCC) classes. The full name of each class can be found from land cover map user guide: http://maps.elie.ucl.ac.be/CCI/viewer/. The underlying data has a resolution of roughly 350 meters (defined in degrees, not meters). The data extracted from GeoQuery corresponds to the count of pixels in each unit (county) associated with each land cover class. One can then multiply each count by the resolution (350m x 350m) to get an approximate coverage estimate in square meters.

Particulate matter ($PM_{2.5}$) estimates are based on prediction models that combine satellite-based estimates and simulations based on the TM5-FASST model, an atmospheric source–receptor model that analyses emission changes of air quality and short-lived climate pollutants (see Van Dingenen et al., 2018).

[23] https://www.aiddata.org/geoquery.

[24] The steradian (sr) is a unit derived from the meter (m). Its expression, in base units, is $sr = m^2 \cdot m^{-2}$. It is thus a dimensionless unit. The energy intensity is expressed in watt per steradian and the radiance, in watt per square meter steradian. The original data in the AidData geoquery tool was in $nanoWatt/cm^2/sr$ and has been converted in $Watt/km^2/sr$.

[25] Figure 1 represents the continental United States at night and is a composite assembled from data acquired by the Suomi NPP satellite in April and October 2012. The image was made possible by the satellite's "Day/Night Band" of the Visible Infrared Imaging Radiometer Suite (VIIRS), which detects light in a range of wavelengths from green to near-infrared and uses filtering techniques to observe dim signals such as city lights, gas flares, auroras, wildfires and reflected moonlight. Credit: NASA Earth Observatory/NOAA NGDC.

[26] See http://Aiddata.org/geoquery and https://www.esa-landcover-cci.org

A.2. County GDP & Population

Data on yearly county-level domestic product (GDP) were extracted from the Bureau of Economic Analysis' web site: GDP by County, Metro, and Other Areas. GDP is measured by the income approach, *i.e.* as the sum of compensation of employees, taxes on production and imports less subsidies (SUB), and gross operating surpluses. Details of the procedure can be found in Aysheshim et al. (2020).

Yearly county-level population estimates were drawn from the Census Bureau's web site: https://www.census.gov/data/datasets/time-series/demo/popest/2010s-counties-total.html. Naturally, intercensal population counts are not available and must be estimated. The Census Bureau uses a procedure that has been shown to be very accurate in the past (see Yowell and Devine, 2013). The details of the procedure can be found here.

References

Addison, D.M., Stewart, B., 2015. Nighttime lights revisited: the use of nighttime lights data as a proxy for economic variables. Technical Report 7496. World Bank Policy Research Working Paper.

Ahn, S.C., Horenstein, A.R., 2013. Eigenvalue ratio test for the number of factors. Econometrica 81, 1203–1227.

Aysheshim, K.D., Hinson, J.R., Panek, S.D., 2020. A primer on local area gross domestic product methodology. Survey of Current Business 100, 1–13.

Bai, J., Ng, S., 2002. Determining the number of factors in approximate factor models. Econometrica 70, 191–221.

Bickenbach, F., Bode, E., Nunnenkamp, P., Söder, M., 2016. Night lights and regional GDP. Review of World Economics 152, 425–447.

Blundell, R., Bond, S., Meghir, C., 1996. Econometric models of company investment, in: Matyas, L., Sevestre, P. (Eds.), The Econometrics of Panel Data. A Handbook of the Theory with Applications, second revised edition. Springer, pp. 685–710.

Bondy, M., Roth, S., Sager, L., 2020. Crime is in the air: the contemporaneous relationship between air pollution and crime. Journal of the Association of Environmental and Resource Economists. 7, 555–585.

Bresson, G., Kramarz, F., Sevestre, P., 1996. Dynamic labour demand models, in: Matyas, L., Sevestre, P. (Eds.), The Econometrics of Panel Data. A Handbook of the Theory with Applications, second revised edition. Springer, pp. 660–684.

Brueckner, J.K., 2003. Strategic interaction among governments: An overview of empirical studies. International Regional Science Review 26, 175–188.

Burkhardt, J., Bayham, J., Wilson, A., Carter, E., Berman, J.D., O'Dell, K., Ford, B., Fischer, E.V., Pierce, J.R., 2019. The effect of pollution on crime: Evidence from data on particulate matter and ozone. Journal of Environmental Economics and Management 98, 102267.

Burns, A.C., Saxena, R., Vetter, C., Phillips, A.J., Lane, J.M., Cain, S.W., 2021. Time spent in outdoor light is associated with mood, sleep, and circadian rhythm-related outcomes: A cross-sectional and longitudinal study in over 400,000 UK Biobank participants. Journal of Affective Disorders 295, 347–352.

Cain, S.W., McGlashan, E.M., Vidafar, P., Mustafovska, J., Curran, S.P., Wang, X., Mohamed, A., Kalavally, V., Phillips, A.J., 2020. Evening home lighting adversely impacts the circadian system and sleep. Scientific Reports 10, 1–10.

Cattell, R.B., 1966. The scree test for the number of factors. Multivariate Behavioral Research 1, 245–276.

Ch, R., Martin, D.A., Vargas, J.F., 2021. Measuring the size and growth of cities using nighttime light. Journal of Urban Economics 125, 103254.

Chalfin, A., Hansen, B., Lerner, J., Parker, L., 2022. Reducing crime through environmental design: Evidence from a randomized experiment of street lighting in new york city. Journal of Quantitative Criminology 38, 127–157.

Chen, X., Nordhaus, W.D., 2011. Using luminosity data as a proxy for economic statistics. Proceedings of the National Academy of Sciences 108, 8589–8594.

Chen, X., Nordhaus, W.D., 2019. VIIRS nighttime lights in the estimation of cross-sectional and time-series GDP. Remote Sensing 11, 1057.

CIRES, 2011. Bright city lights exacerbate air pollution. Spheres , 4–5.URL: http://www.jstor.org/stable/24352775.

Debarsy, N., Ertur, C., LeSage, J.P., 2012. Interpreting dynamic space–time panel data models. Statistical Methodology 9, 158–171.

Ditzen, J., Reese, S., 2023. xtnumfac: A battery of estimators for the number of common factors in time series and panel-data models. The Stata Journal 23, 438–454.

Dizon, E., Pranggono, B., 2022. Smart streetlights in smart city: a case study of Sheffield. Journal of Ambient Intelligence and Humanized Computing , 1–16.

Doleac, J.L., Sanders, N.J., 2015. Under the cover of darkness: How ambient light influences criminal activity. The Review of Economics and Statistics 97, 1093–1103.

Duriscoe, D., Luginbuhl, C., Elvidge, C., 2014. The relation of outdoor lighting characteristics to sky glow from distant cities. Lighting Research & Technology 46, 35–49.

Elhorst, J.P., 2014. Spatial panel data models, in: Elhorst, J.P. (Ed.), Spatial Econometrics, From Cross-Sectional Data to Spatial Panels. Springer, pp. 37–93.

Elhorst, J.P., 2021. The dynamic general nesting spatial econometric model for spatial panels with common factors: Further raising the bar. Review of Regional Research , 1–19.

Elvidge, C.D., Baugh, K., Zhizhin, M., Hsu, F.C., Ghosh, T., 2017. VIIRS nighttime lights. International Journal of Remote Sensing 38, 5860–5879.

Elvidge, C.D., Zhizhin, M., Ghosh, T., Hsu, F.C., Taneja, J., 2021. Annual time series of global VIIRS nighttime lights derived from monthly averages: 2012 to 2019. Remote Sensing 13, 922.

European Commission, 2021. A European Green Deal. Striving to be the first climate-neutral continent. European Commission.

Falchi, F., Cinzano, P., Duriscoe, D., Kyba, C.C., Elvidge, C.D., Baugh, K., Portnov, B.A., Rybnikova, N.A., Furgoni, R., 2016. The new world atlas of artificial night sky brightness. Science Advances 2, e1600377.

Gallaway, T., Olsen, R.N., Mitchell, D.M., 2010. The economics of global light pollution. Ecological Economics 69, 658–665.

Gibson, J., Boe-Gibson, G., 2021. Nighttime lights and county-level economic activity in the United States: 2001 to 2019. Remote Sensing 13, 2741.

Glaeser, E.L., Gottlieb, J.D., 2009. The wealth of cities: Agglomeration economies and spatial equilibrium in the United States. Journal of Economic Literature 47, 983–1028.

Glaeser, E.L., Scheinkman, J., Shleifer, A., 1995. Economic growth in a cross-section of cities. Journal of Monetary Economics 36, 117–143.

Goldblatt, R., Heilmann, K., Vaizman, Y., 2020. Can medium-resolution satellite imagery measure economic activity at small geographies? Evidence from Landsat in Vietnam. The World Bank Economic Review 34, 635–653.

Goodman, S., BenYishay, A., Lv, Z., Runfola, D., 2019. Geoquery: Integrating HPC systems and public web-based geospatial data tools. Computers & Geosciences 122, 103–112.

Goulet, G., Mongrain, V., Desrosiers, C., Paquet, J., Dumont, M., 2007. Daily light exposure in morning-type and evening-type individuals. Journal of Biological Rhythms 22, 151–158.

Henderson, J.V., Storeygard, A., Weil, D.N., 2012. Measuring economic growth from outer space. American Economic Review 102, 994–1028.

Henderson, V., Storeygard, A., Weil, D.N., 2011. A bright idea for measuring economic growth. American Economic Review 101, 194–99.

Hendry, D.F., Pagan, A.R., Sargan, J.D., 1984. Dynamic specification, in: Griliches, Z., Intriligator, M.D. (Eds.), Handbook of Econometrics. volume 2, pp. 1023–1100.

Herrnstadt, E., Heyes, A., Muehlegger, E., Saberian, S., 2021. Air pollution and criminal activity: Microgeographic evidence from chicago. American Economic Journal: Applied Economics 13, 70–100.

Hu, Y., Yao, J., 2022. Illuminating economic growth. Journal of Econometrics 228, 359–378.

Im, K.S., Pesaran, M.H., Shin, Y., 2003. Testing for unit roots in heterogeneous panels. Journal of Econometrics 115, 53–74.

Jewett, M.E., Kronauer, R.E., Czeisler, C.A., 1994. Phase-amplitude resetting of the human circadian pacemaker via bright light: a further analysis. Journal of Biological Rhythms 9, 295–314.

Jones, B.A., 2022. Dust storms and violent crime. Journal of Environmental Economics and Management 111, 102590.

Juodis, A., Reese, S., 2022. The incidental parameters problem in testing for remaining cross-section correlation. Journal of Business & Economic Statistics 40, 1191–1203.

Kennan, J., 1979. The estimation of partial adjustment models with rational expectations. Econometrica , 1441–1455.

Keola, S., Andersson, M., Hall, O., 2015. Monitoring economic development from space: using nighttime light and land cover data to measure economic growth. World Development 66, 322–334.

Kuo, P.F., Putra, I.G.B., 2021. Analyzing the relationship between air pollution and various types of crime. PLoS One 16, e0255653.

Kyba, C.C., Kuester, T., Sánchez de Miguel, A., Baugh, K., Jechow, A., Hölker, F., Bennie, J., Elvidge, C.D., Gaston, K.J., Guanter, L., 2017. Artificially lit surface of Earth at night increasing in radiance and extent. Science Advances 3, e1701528.

Lee, L.F., Yu, J., 2015. Spatial panel data models, in: Baltagi, B.H. (Ed.), The Oxford Handbook of Panel Data. Oxford University Press, pp. 363–401.

LeSage, J., Pace, R., 2009. An Introduction to Spatial Econometrics. CRC Press, Taylor-Francis.

Martinez-Nicolas, A., Martinez-Madrid, M.J., Almaida-Pagan, P.F., Bonmati-Carrion, M.A., Madrid, J.A., Rol, M.A., 2019. Assessing chronotypes by ambulatory circadian monitoring. Frontiers in Physiology 10, 1396.

Mitre-Becerril, D., Tahamont, S., Lerner, J., Chalfin, A., 2022. Can deterrence persist? long-term evidence from a randomized experiment in street lighting. Criminology & Public Policy 21, 865–891.

Onatski, A., 2010. Determining the number of factors from empirical distribution of eigenvalues. The Review of Economics and Statistics 92, 1004–1016.

Parent, O., LeSage, J.P., 2011. A space-time filter for panel data models containing random effects. Computational Statistics & Data Analysis 55, 475–490.

Pesaran, M.H., 2004. General diagnostic tests for cross section dependence in panels. Technical Report. Institute for the Study of Labor (IZA) Discussion Paper No. 1240.

Pesaran, M.H., 2007. A simple panel unit root test in the presence of cross-section dependence. Journal of Applied Econometrics 22, 265–312.

Pesaran, M.H., Xie, Y., 2021. A bias-corrected CD test for error cross-sectional dependence in panel data models with latent factors. Technical Report. arXiv preprint arXiv:2109.00408.

Sager, L., 2019. Estimating the effect of air pollution on road safety using atmospheric temperature inversions. Journal of Environmental Economics and Management 98, 102250.

Ścięż̇or, T., Czaplicka, A., 2020. The impact of atmospheric aerosol particles on the brightness of the night sky. Journal of Quantitative Spectroscopy and Radiative Transfer 254, 107168.

Shi, W., Lee, L.f., 2017. Spatial dynamic panel data models with interactive fixed effects. Journal of Econometrics 197, 323–347.

Firmino Costa da Silva, D., Elhorst, J.P., Silveira Neto, R.d.M., 2017. Urban and rural population growth in a spatial panel of municipalities. Regional Studies 51, 894–908.

Stark, H., Brown, S., Wong, K., Stutz, J., Elvidge, C., Pollack, I., Ryerson, T., Dube, W., Wagner, N., Parrish, D., 2011. City lights and urban air. Nature Geoscience 4, 730–731.

Tompson, L., Steinbach, R., Johnson, S., 2022. Absence of street lighting may prevent vehicle crime, but spatial and temporal displacement remains a concern. Journal of Quantitative Criminology , 1–21.

Van Dingenen, R., Dentener, F., Crippa, M., Leitao, J., Marmer, E., Rao, S., Solazzo, E., Valentini, L., 2018. TM5-FASST: A global atmospheric source–receptor model for rapid impact analysis of emission changes on air quality and short-lived climate pollutants. Atmospheric Chemistry and Physics 18, 16173–16211.

Yowell, T., Devine, J., 2013. Evaluating current and alternative methods to produce 2010 county population estimates. Census Bureau Working Paper Number POP-WP100.

Yu, J., De Jong, R., Lee, L.F., 2008. Quasi-maximum likelihood estimators for spatial dynamic panel data with fixed effects when both n and T are large. Journal of Econometrics 146, 118–134.

Zhao, M., Zhou, Y., Li, X., Cao, W., He, C., Yu, B., Li, X., Elvidge, C.D., Cheng, W., Zhou, C., 2019. Applications of satellite remote sensing of nighttime light observations: Advances, challenges, and perspectives. Remote Sensing 11, 1971.

Nighttime light pollution and economic activities: a spatio-temporal model with common factors for US counties
Supplementary material

Georges Bresson[a], Jean-Michel Etienne[b], Guy Lacroix[c,*]

[a] *Department of Economics, Université Paris Panthéon-Assas, France*
[b] *Department of Economics, University Paris Sud, France*
[c] *Department of Economics, Université Laval, Québec, QC, Canada*

July 24, 2023

Contents

*Corresponding author. Department of Economics, Pavillon J.-A.-DeSève, 1025, avenue des Sciences-Humaines, Université Laval, Québec (Québec) G1V 0A6, Canada.

Email addresses: georges.bresson@u-paris2.fr (Georges Bresson), jean-michel.etienne@u-psud.fr (Jean-Michel Etienne), Guy.Lacroix@ecn.ulaval.ca (Guy Lacroix)

A. Derivation of the spatial urban model of nighttime lights pollution and economic activities

The first-order conditions of profit maximisation:

$$\begin{aligned} \max \pi_{it} &= Q_{it} - p_{K_{it}} K_{it} - p_{\overline{Z}_i} \overline{Z}_i - s_{it} L_{it} \\ &= A_{it} L_{it}^{\beta_L} K_{it}^{\beta_K} \overline{Z}_i^{1-\beta_L-\beta_K} - K_{it} - \overline{Z}_i - s_{it} L_{it} \end{aligned} \tag{A.1}$$

lead to

$$\left\{ \begin{array}{rcll} \frac{\partial \pi_{it}}{\partial L_{it}} & = & s_{it} & = A_{it} \beta_L L_{it}^{\beta_L - 1} K_{it}^{\beta_K} \overline{Z}_i^{1-\beta_L-\beta_K} \\ \frac{\partial \pi_{it}}{\partial K_{it}} & = & 1 & = A_{it} \beta_K L_{it}^{\beta_L} K_{it}^{\beta_K - 1} \overline{Z}_i^{1-\beta_L-\beta_K} \end{array} \right.$$

and

$$\begin{aligned} s_{it} &= A_{it} \beta_L L_{it}^{\beta_L - 1} \left[A_{it} \beta_K L_{it}^{\beta_L} \overline{Z}_i^{1-\beta_L-\beta_K} \right]^{\frac{\beta_K}{1-\beta_K}} \overline{Z}_i^{1-\beta_L-\beta_K} \\ &= A_{it}^{\frac{1}{1-\beta_K}} \beta_L \beta_K^{\frac{\beta_K}{1-\beta_K}} L_{it}^{\frac{\beta_L+\beta_K-1}{1-\beta_K}} \overline{Z}_i^{\frac{1-\beta_L-\beta_K}{1-\beta_K}} \end{aligned} \tag{A.2}$$

The first-order conditions of utility maximisation, subject to the budget constraint:

$$\begin{aligned} \max \mathbb{L}_{it} = {} & C_{it}^{1-\alpha} H_{it}^{\alpha} \left(R_{it}^{-\psi} \prod_{j(\neq i)=1}^{N} R_{jt}^{-\zeta w_{ij}} \right) \left(P_{it}^{-\kappa} \prod_{j(\neq i)=1}^{N} P_{jt}^{-\xi w_{ij}} \right) L_{it}^{-\varphi} \prod_{j(\neq i)=1}^{N} L_{jt}^{-\nu w_{ij}} \\ & - \lambda \left(C_{it} + p_{H_{it}} H_{it} - s_{it} L_{it} \right) \end{aligned}$$

lead to

$$\left\{ \begin{array}{rcl} \frac{\partial \mathbb{L}_{it}}{\partial C_{it}} & = & (1-\alpha) C_{it}^{-\alpha} H_{it}^{\alpha} \left(R_{it}^{-\psi} \prod_{j(\neq i)=1}^{N} R_{jt}^{-\zeta w_{ij}} \right) \left(P_{it}^{-\kappa} \prod_{j(\neq i)=1}^{N} P_{jt}^{-\xi w_{ij}} \right) L_{it}^{-\varphi} \prod_{j(\neq i)=1}^{N} L_{jt}^{-\nu w_{ij}} - \lambda = 0 \\ \frac{\partial \mathbb{L}_{it}}{\partial H_{it}} & = & \alpha C_{it}^{1-\alpha} H_{it}^{\alpha-1} \left(R_{it}^{-\psi} \prod_{j(\neq i)=1}^{N} R_{jt}^{-\zeta w_{ij}} \right) \left(P_{it}^{-\kappa} \prod_{j(\neq i)=1}^{N} P_{jt}^{-\xi w_{ij}} \right) L_{it}^{-\varphi} \prod_{j(\neq i)=1}^{N} L_{jt}^{-\nu w_{ij}} - \lambda p_{H_{it}} = 0 \end{array} \right.$$

and

$$\frac{\frac{\partial \mathbb{L}_{it}}{\partial H_{it}}}{\frac{\partial \mathbb{L}_{it}}{\partial C_{it}}} = \frac{\alpha C_{it}^{1-\alpha} H_{it}^{\alpha-1}}{(1-\alpha) C_{it}^{-\alpha} H_{it}^{\alpha}} = \frac{\alpha C_{it} H_{it}^{-1}}{1-\alpha} = p_{H_{it}} \ \rightarrow \ p_{H_{it}} H_{it} = \left(\frac{\alpha}{1-\alpha} \right) C_{it}$$

Since

$$\begin{aligned} C_{it} + p_{H_{it}} H_{it} &= s_{it} L_{it} \\ p_{H_{it}} H_{it} &= s_{it} L_{it} - C_{it} \\ \left(\frac{\alpha}{1-\alpha} \right) C_{it} &= s_{it} L_{it} - C_{it} \\ C_{it} &= (1-\alpha) s_{it} L_{it} \end{aligned}$$

then

$$\begin{aligned} p_{H_{it}} H_{it} &= \left(\frac{\alpha}{1-\alpha}\right) C_{it} = \left(\frac{\alpha}{1-\alpha}\right)(1-\alpha)\, s_{it} L_{it} \\ H_{it} &= \frac{\alpha s_{it} L_{it}}{p_{H_{it}}} \end{aligned}$$

As $C_{it} = (1-\alpha)\, s_{it} L_{it}$, the indirect utility function is given by

$$\begin{aligned} V_t &= C_{it}^{1-\alpha} H_{it}^{\alpha} \left(R_{it}^{-\psi} \prod_{j(\neq i)=1}^{N} R_{jt}^{-\zeta w_{ij}}\right)\left(P_{it}^{-\kappa} \prod_{j(\neq i)=1}^{N} P_{jt}^{-\xi w_{ij}}\right) L_{it}^{-\varphi} \prod_{j(\neq i)=1}^{N} L_{jt}^{-\nu w_{ij}} \\ &= (1-\alpha)^{1-\alpha}\, s_{it}^{1-\alpha} L_{it}^{1-\alpha} \left(\frac{\alpha s_{it} L_{it}}{p_{H_{it}}}\right)^{\alpha} \left(R_{it}^{-\psi} \prod_{j(\neq i)=1}^{N} R_{jt}^{-\zeta w_{ij}}\right)\left(P_{it}^{-\kappa} \prod_{j(\neq i)=1}^{N} P_{jt}^{-\xi w_{ij}}\right) L_{it}^{-\varphi} \prod_{j(\neq i)=1}^{N} L_{jt}^{-\nu w_{ij}} \\ &= \alpha^{\alpha} (1-\alpha)^{1-\alpha}\, s_{it} p_{H_{it}}^{-\alpha} \left(R_{it}^{-\psi} \prod_{j(\neq i)=1}^{N} R_{jt}^{-\zeta w_{ij}}\right)\left(P_{it}^{-\kappa} \prod_{j(\neq i)=1}^{N} P_{jt}^{-\xi w_{ij}}\right) L_{it}^{1-\varphi} \prod_{j(\neq i)=1}^{N} L_{jt}^{-\nu w_{ij}} \end{aligned} \tag{A.3}$$

Differentiating the profit function $\pi_{it} = p_{H_{it}} hl - c_0 h^{\delta} l - p_l l$ with respect to height (h) and solving the resulting first-order condition, yields:

$$\frac{\partial \pi_{it}}{\partial h} = p_{H_{it}} l - \delta c_0 h^{\delta-1} l = 0 \;\rightarrow\; h = \left(\frac{p_{H_{it}}}{\delta c_0}\right)^{\frac{1}{\delta-1}}$$

which implies that housing supply is given by

$$hl = \left(\frac{p_{H_{it}}}{\delta c_0}\right)^{\frac{1}{\delta-1}} l$$

By comparing housing demand with housing supply leads to the housing price equation:

$$\begin{aligned} H_{it} &= hl \\ \frac{\alpha s_{it} L_{it}}{p_{H_{it}}} &= \left(\frac{p_{H_{it}}}{\delta c_0}\right)^{\frac{1}{\delta-1}} l \\ \alpha s_{it} L_{it} &= p_{H_{it}} \left(\frac{p_{H_{it}}}{\delta c_0}\right)^{\frac{1}{\delta-1}} l = p_{H_{it}}^{\frac{\delta}{\delta-1}} (\delta c_0)^{\frac{-1}{\delta-1}} l \\ p_{H_{it}}^{\frac{\delta}{\delta-1}} &= \frac{\alpha s_{it} L_{it}}{l\,(\delta c_0)^{\frac{-1}{\delta-1}}} \\ p_{H_{it}} &= \left(\frac{\alpha s_{it} L_{it}}{l}\right)^{\frac{\delta-1}{\delta}} (\delta c_0)^{\frac{1}{\delta}} \end{aligned} \tag{A.4}$$

The system formed by labour demand (A.2), indirect utility (A.3) and housing prices

(A.4) is given by:

$$\begin{cases} s_{it} &= A_{it}^{\frac{1}{1-\beta_K}} \beta_L \beta_K^{\frac{\beta_K}{1-\beta_K}} L_{it}^{\frac{\beta_L+\beta_K-1}{1-\beta_K}} \overline{Z}_i^{\frac{1-\beta_L-\beta_K}{1-\beta_K}} \\ V_t &= \alpha^\alpha (1-\alpha)^{1-\alpha} s_{it} p_{H_{it}}^{-\alpha} \left(R_{it}^{-\psi} \prod_{j(\neq i)=1}^{N} R_{jt}^{-\zeta w_{ij}} \right) \left(P_{it}^{-\kappa} \prod_{j(\neq i)=1}^{N} P_{jt}^{-\xi w_{ij}} \right) L_{it}^{1-\varphi} \prod_{j(\neq i)=1}^{N} L_{jt}^{-\nu w_{ij}} \\ p_{H_{it}} &= \left(\frac{\alpha s_{it} L_{it}}{l} \right)^{\frac{\delta-1}{\delta}} (\delta c_0)^{\frac{1}{\delta}} \end{cases}$$

Taking logarithms, we get

$$\begin{cases} \log s_{it} &= \log \beta_L + \frac{\beta_K}{1-\beta_K} \log \beta_K + \frac{1}{1-\beta_K} \log A_{it} + \frac{\beta_L+\beta_K-1}{1-\beta_K} \log L_{it} + \frac{1-\beta_L-\beta_K}{1-\beta_K} \log \overline{Z}_i \\ \log V_t &= \begin{cases} \alpha \log \alpha + (1-\alpha) \log (1-\alpha) + \log s_{it} - \alpha \log p_{H_{it}} - \psi \log R_{it} - \sum_{j(\neq i)=1}^{N} \zeta w_{ij} \log R_{jt} \\ -\kappa \log P_{it} - \sum_{j(\neq i)=1}^{N} \xi w_{ij} \log P_{jt} + (1-\varphi) \log L_{it} - \sum_{j(\neq i)=1}^{N} \nu w_{ij} \log L_{jt} \end{cases} \\ \log p_{H_{it}} &= \frac{\delta-1}{\delta} (\log \alpha + \log s_{it} + \log L_{it} - \log l) + \frac{1}{\delta} \log (\delta c_0) \end{cases}$$

Then,

$$\begin{aligned} \log V_t &= \alpha \log \alpha + (1-\alpha) \log (1-\alpha) + \log \beta_L + \frac{\beta_K}{1-\beta_K} \log \beta_K + \frac{1}{1-\beta_K} \log A_{it} \\ &+ \frac{\beta_L+\beta_K-1}{1-\beta_K} \log L_{it} + \frac{1-\beta_L-\beta_K}{1-\beta_K} \log \overline{Z}_i \\ &- \frac{\alpha(\delta-1)}{\delta} \left(\begin{array}{c} \log \alpha + \log \beta_L + \frac{\beta_K}{1-\beta_K} \log \beta_K + \frac{1}{1-\beta_K} \log A_{it} \\ + \frac{\beta_L+\beta_K-1}{1-\beta_K} \log L_{it} + \frac{1-\beta_L-\beta_K}{1-\beta_K} \log \overline{Z}_i \\ + \log L_{it} - \log l \end{array} \right) - \frac{\alpha}{\delta} \log (\delta c_0) \\ &- \psi \log R_{it} - \sum_{j(\neq i)=1}^{N} \zeta w_{ij} \log R_{jt} - \kappa \log P_{it} - \sum_{j(\neq i)=1}^{N} \xi w_{ij} \log P_{jt} \\ &+ (1-\varphi) \log L_{it} - \sum_{j(\neq i)=1}^{N} \nu w_{ij} \log L_{jt} \end{aligned}$$

and

$$\log R_{it} = \frac{1}{\psi} \left[\begin{array}{c} + \left\{ \frac{\delta(1-\alpha)+\alpha}{\delta(1-\beta_K)} \right\} \log A_{it} + \Theta \log L_{it} - \sum_{j(\neq i)=1}^{N} \nu w_{ij} \log L_{jt} \\ - \sum_{j(\neq i)=1}^{N} \zeta w_{ij} \log R_{jt} - \kappa \log P_{it} - \sum_{j(\neq i)=1}^{N} \xi w_{ij} \log P_{jt} + \Phi_{it} \end{array} \right]$$

with

$$\Theta = \frac{\delta(\beta_L+\beta_K-1) - \alpha(\delta-1) + (1-\varphi)(1-\beta_K)}{\delta(1-\beta_K)}$$

and

$$\begin{aligned}\Phi_{it} &= \frac{1}{\delta}\log\alpha + (1-\alpha)\log(1-\alpha) + \frac{\delta-\alpha\delta+1}{\delta}\log\beta_L + \frac{\delta\beta_K - \alpha(\delta-1)}{\delta(1-\beta_K)}\log\beta_K \\ &+ \frac{(1-\beta_L-\beta_K)(\delta(1-\alpha)+\alpha)}{\delta(1-\beta_K)}\log\overline{Z}_i + \frac{\alpha(\delta-1)}{\delta}\log l - \frac{\alpha}{\delta}\log(\delta c_0) - \log V_t\end{aligned}$$

Φ_{it} is a rather cumbersome function of individual specific effects through $\log\overline{Z}_i$ and time effects through $\log V_t$.

Derivation of the logarithm of the TFP

From the Cobb-Douglas production function:

$$Q_{it} = A_{it}L_{it}^{\beta_L}K_{it}^{\beta_K}\overline{Z}_i^{1-\beta_L-\beta_K}$$

we have

$$A_{it} = Q_{it}L_{it}^{-\beta_L}K_{it}^{-\beta_K}\overline{Z}_i^{\beta_L+\beta_K-1}$$

From the first-order conditions of profit maximization (A.1), we get

$$K_{it}^{-\beta_K} = \left(\frac{1}{\beta_K}\right)^{-\frac{\beta_K}{\beta_K-1}} A_{it}^{\frac{\beta_K}{\beta_K-1}} L_{it}^{\frac{\beta_L\beta_K}{\beta_K-1}} \overline{Z}_i^{\frac{\beta_K(1-\beta_L-\beta_K)}{\beta_K-1}}$$

then,

$$A_{it} = Q_{it}^{1-\beta_K}L_{it}^{-\beta_L}\varpi_i \text{ with } \varpi_i = \left(\frac{1}{\beta_K}\right)^{\beta_K}\overline{Z}_i^{\beta_L+\beta_K-1} \tag{A.5}$$

From

$$A_{it} = a_{it}\prod_{j(\neq i)=1}^{N} a_{jt}^{\eta w_{ij}}$$

we can write

$$\begin{aligned}a_{1t} &= A_{1t}\prod_{j(\neq 1)=1}^{N} a_{jt}^{-\eta w_{1j}} \\ &= A_{1t}\left[A_{2t}^{-\eta w_{12}}\prod_{k(\neq 2)=1}^{N} a_{kt}^{\eta^2 w_{12}w_{2k}}\right]\left[A_{3t}^{-\eta w_{13}}\prod_{k(\neq 3)=1}^{N} a_{kt}^{\eta^2 w_{13}w_{3k}}\right]...\end{aligned}$$

then,

$$\begin{aligned} a_{it} &= A_{it} \prod_{j(\neq i)=1}^{N} A_{jt}^{-\eta w_{ij}} a_{jt}^{\eta^2 \left(\sum_{k(\neq j)=1}^{N} w_{kj} w_{ik} \right)} \\ a_{it} \prod_{j(\neq i)=1}^{N} a_{jt}^{\eta w_{ij}} &= A_{it} \prod_{j(\neq i)=1}^{N} A_{jt}^{-\eta w_{ij}} a_{jt}^{\eta w_{ij} + \eta^2 \left(\sum_{k(\neq j)=1}^{N} w_{kj} w_{ik} \right)} \\ &= A_{it} \prod_{j(\neq i)=1}^{N} A_{jt}^{-\eta w_{ij}} \vartheta_{ijt} \end{aligned} \tag{A.6}$$

Substituting (A.5) in (A.6) leads to

$$a_{it} \prod_{j(\neq i)=1}^{N} a_{jt}^{\eta w_{ij}} = Q_{it}^{1-\beta_K} L_{it}^{-\beta_L} \varpi_i \prod_{j(\neq i)=1}^{N} Q_{jt}^{(\beta_K - 1)\eta w_{ij}} L_{jt}^{\beta_L \eta w_{ij}} \varpi_j^{-\eta w_{ij}} \vartheta_{ijt}$$

and

$$\begin{aligned} \log A_{it} &= (1-\beta_K) \log Q_{it} - \beta_L \log L_{it} + \sum_{j(\neq i)=1}^{N} (\beta_K - 1) \eta w_{ij} \log Q_{jt} \\ &\quad + \sum_{j(\neq i)=1}^{N} \beta_L \eta w_{ij} \log L_{jt} + D_{it} \end{aligned}$$

with

$$\begin{aligned} D_{it} &= \log \varpi_i - \sum_{j(\neq i)=1}^{N} \eta w_{ij} \log \varpi_j + \log \vartheta_{ijt} \\ &= \log \varpi_i - \sum_{j(\neq i)=1}^{N} \eta w_{ij} \log \varpi_j \\ &\quad + \sum_{j(\neq i)=1}^{N} \left[\eta w_{ij} + \eta^2 \left(\sum_{k(\neq j)=1}^{N} w_{kj} w_{ik} \right) \log a_{jt} \right] \\ \text{with } \varpi_i &= \left(\frac{1}{\beta_K} \right)^{\beta_K} \overline{Z}_i^{\beta_L + \beta_K - 1} \end{aligned}$$

D_{it} is a rather cumbersome function of individual specific effects through $\log \overline{Z}_i$, $\sum_{j(\neq i)=1}^{N} \log \overline{Z}_j$ and time effects through $\sum_{j(\neq i)=1}^{N} \log a_{jt}$.

B. Unit root tests and figures

Table B1: CIPS unit root tests

	CIPS test	
$\log R$	intercept	-1.718
	intercept and trend	-2.209
$\log Q$	intercept	-2.001
	intercept and trend	-2.432
$\log L$	intercept	-1.919
	intercept and trend	-2.940$^{(*)}$
urban rate	intercept	-0.907
	intercept and trend	-1.410
$\log P$	intercept	-6.032$^{(*)}$
	intercept and trend	-6.334$^{(*)}$

R: radiance, Q: GDP/km^2
L: population density, P : PM2.5 concentration.
H_0: all panels contain unit roots,H_a: some panels are stationary.
Critical values for CIPS ($N = 200$,$T = 10$, Pesaran (2006, 2007)).
Intercept : -2.28 (1%), -2.10 (5%), -2.01 (10%).
Intercept + trend : -2.98 (1%), -2.75 (5%), -2.63 (10%).
(*): the test rejects the null hypothesis of unit roots at the 5% level.

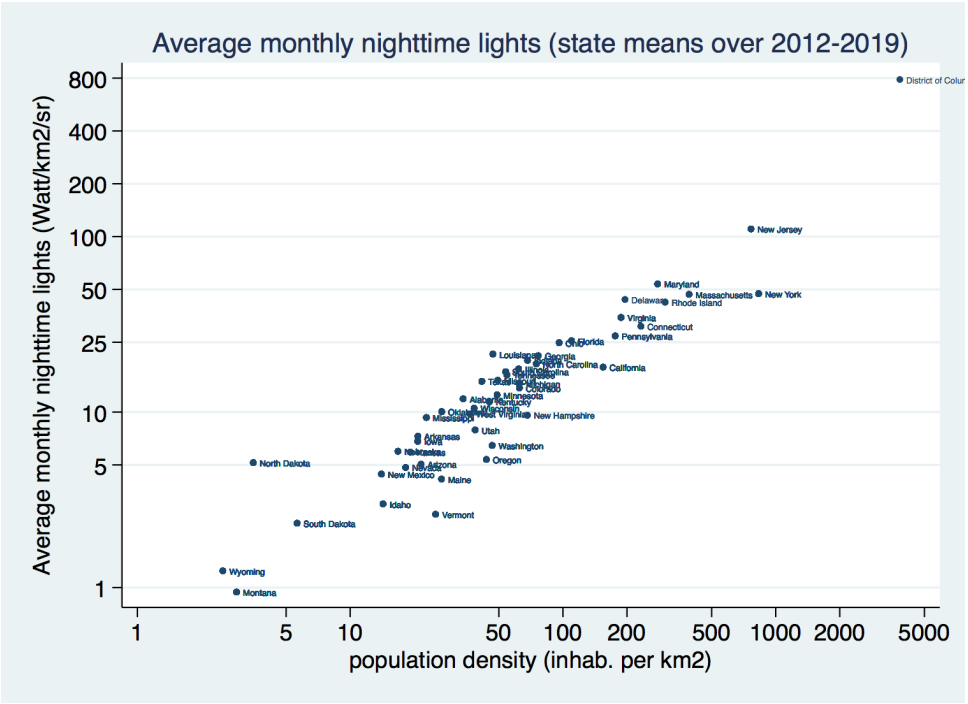

Figure B1: Scatter plot of state averages monthly radiance and population density.

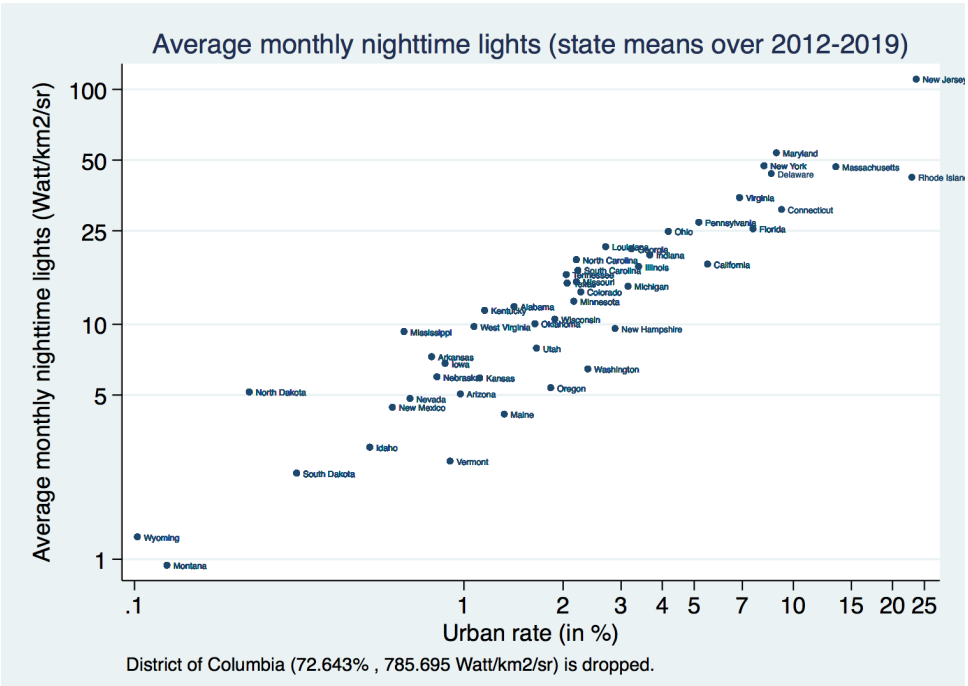

Figure B2: Scatter plot of state averages of monthly radiance and urban rate.

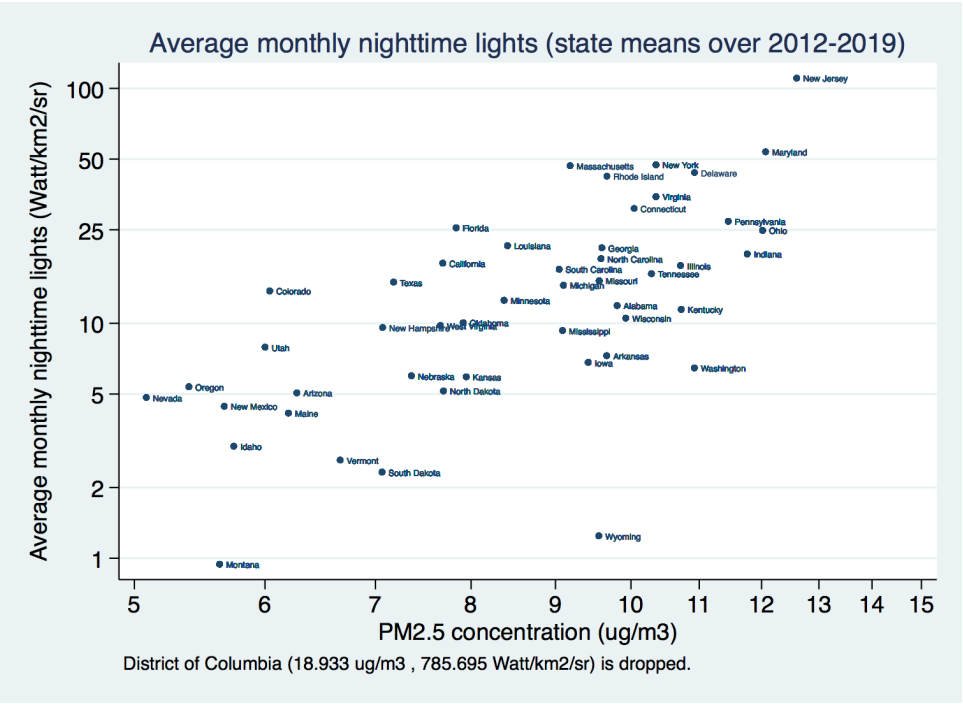

Figure B3: Scatter plot of state averages of monthly radiance and PM25 concentration.

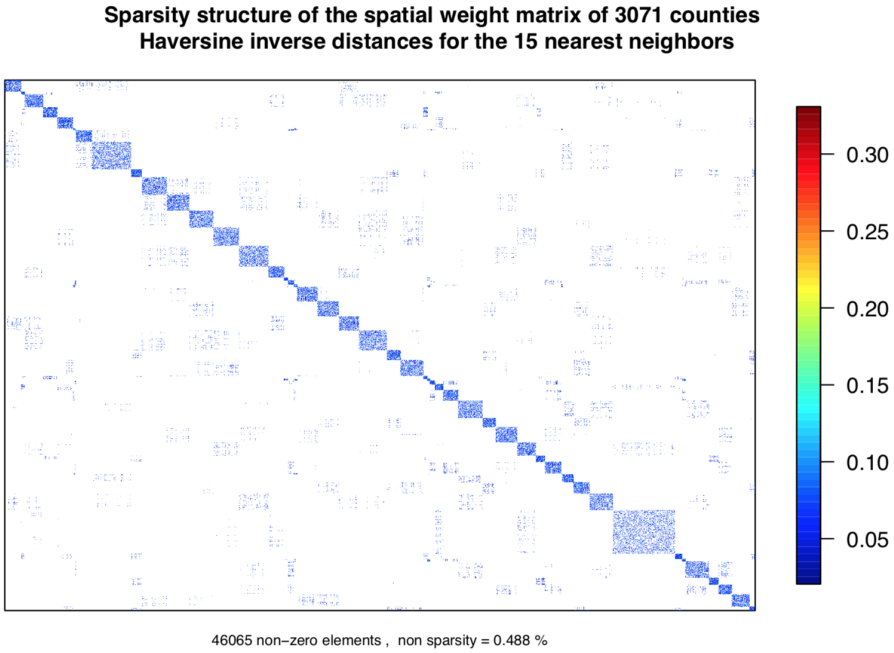

Figure B4: Row-normalized Haversine inverse distance matrix for the 15 nearest neighbors.

C. Number of common factors: Selection methods of Cattell (1966), Onatski (2010) and Ahn and Horenstein (2013)

Cattell (1966)'s approach to determining the number of common factors to include in the regression consists in drawing a scree plot of the eigenvalues of the factors or the principal components. Factors or components located to the left of the "elbow" where the plot levels off are included in the model. In Figure C5, different decision rules are presented. The classical ones are the Kaiser rule, the parallel analysis, and the usual scree test. Non graphical solutions to the Cattell subjective scree test are also proposed: an acceleration factor (AF) and the optimal coordinates index (OC). The acceleration factor indicates where the elbow of the scree plot is located. It corresponds to the acceleration of the curve, *i.e.* the second derivative. The optimal coordinates are the extrapolated coordinates of the previous eigenvalue that allow the observed eigenvalue to go beyond this extrapolation. The Kaiser rule or a parallel analysis criterion (parallel) must also be simultaneously satisfied to retain the components/factors, whether for the acceleration factor, or for the optimal coordinates. Figure C5 shows that $r = 2$ factors could be retained as significant for the matrix of observations $[Y, Z]$ where $Z = [W_N Y, Y_{-1}, W_N Y_{-1}, X, W_N X]$ with $X = [\log Q, \log L,\ \text{urban rate}, \log P]$ and $Y = \log R$.

The eigenvalue ratio method of Ahn and Horenstein (2013) and the eigenvalue difference method of Onatski (2010) are based on ratios and differences of two adjacent eigenvalues of a positive semi-definite matrix. Let A be a $(N \times T)$ matrix of observations. The optimal number of factors of the eigenvalue ratio method $\widehat{r}_{ER}$ is given by $\widehat{r}_{ER} = \min_{0 \leq r \leq r_{max}} \varpi_r / \varpi_{r+1}$, where $\varpi_0 = \sum_{r=1}^{\min(N,T)} \varpi_r / \log \min(N, T)$. And the optimal number of factors of the eigenvalue difference method $\widehat{r}_{ED}$ is given by $\widehat{r}_{ED} = \max \{r \leq r_{max} : \varpi_r - \varpi_{r+1} \geq \delta\}$, where δ is some fixed number. $\varpi_r = \Psi_r(XX'/NT)$ where $\Psi_r(V)$ denotes the rth largest eigenvalue of a positive semi-definite matrix V. Using the matrix of observations $[Y, Z]$, the number of factors from Onatski (2010)'s empirical distribution of eigenvalues (resp. from Ahn and Horenstein (2013)'s eigenvalue ratio method) is $r = 2$ (resp. $r = 1$). We therefore choose $r = 2$ factors for the estimation of the dynamic general nesting spatial panel model with common correlated effects (DGNSP-CCE).

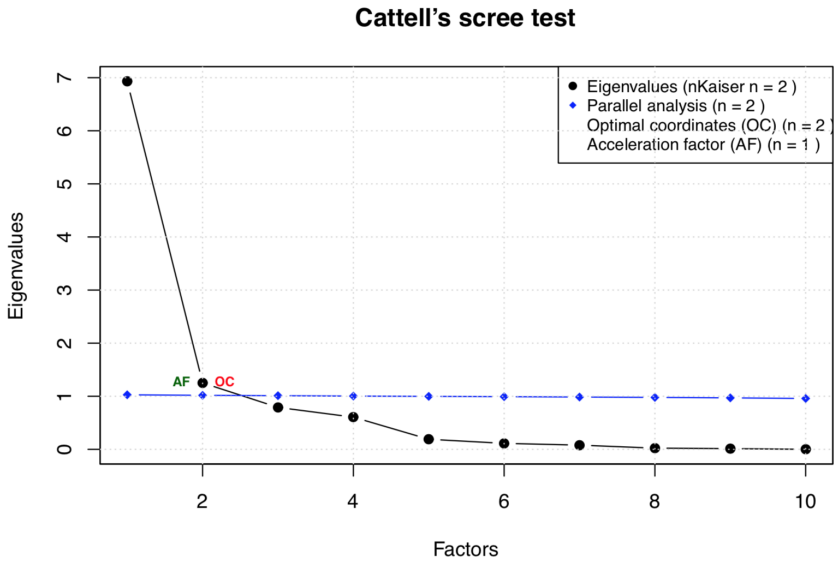

Figure C5: Cattell (1966)'s scree test plot.

D. Results

D.1. Tables and figures

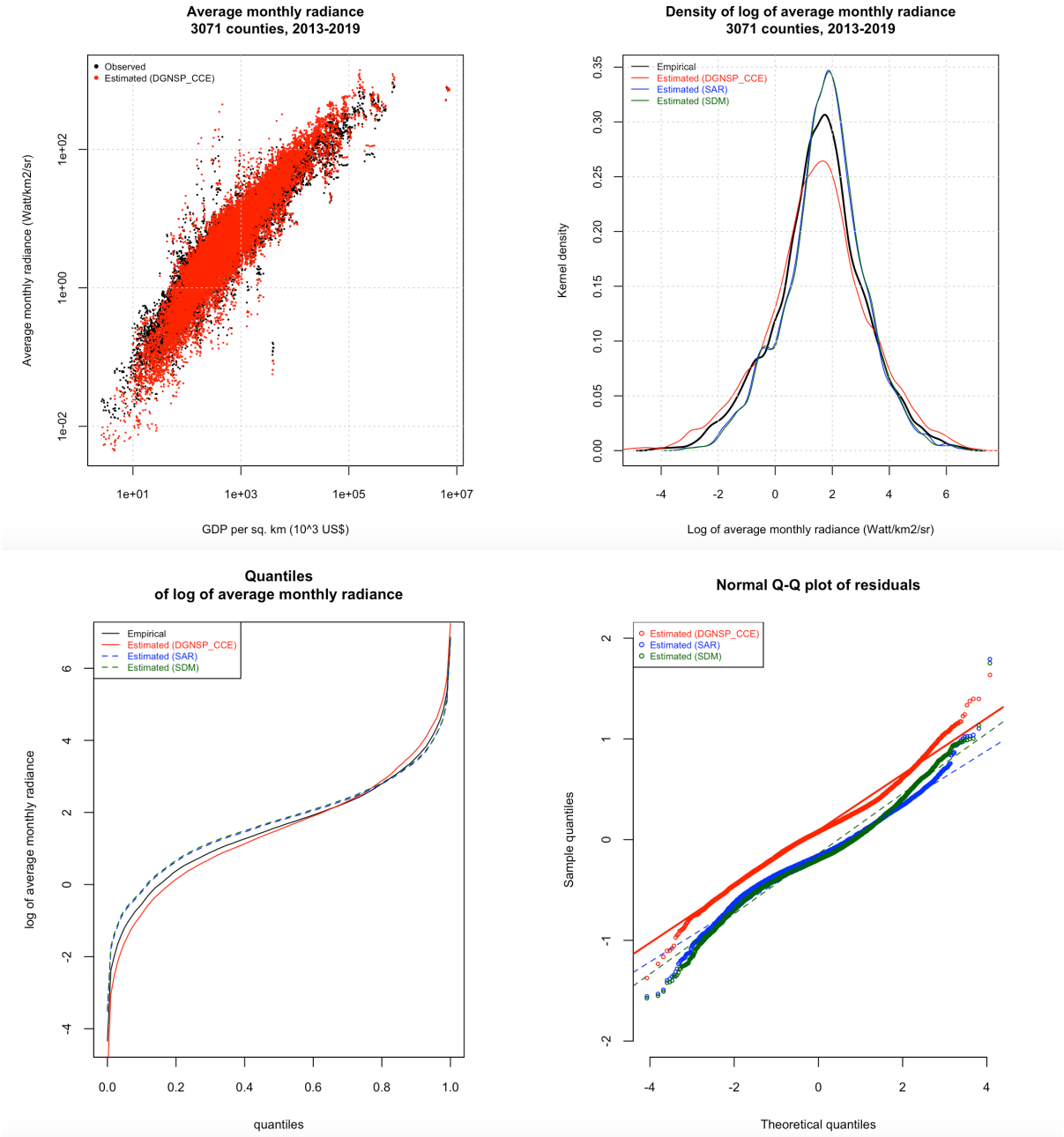

Figure D6: Observed and estimated average monthly radiance. Density, quantiles and Q-Q plot of residuals.

Table D2: IPS and CIPS unit root tests on residuals

	CIPS	test	IPS	test	p-value
DGNSP-CCE	intercept	-2.234$^{(*)}$	demean	-71.839	0.000
	intercept and trend	-2.546	demean and trend	-56.356	0.000
DSAR	intercept	-2.362$^{(*)}$	demean	-98.653	0.000
	intercept and trend	-3.068$^{(*)}$	demean and trend	-63.091	0.000
DSDM	intercept	-2.370$^{(*)}$	demean	-98.334	0.000
	intercept and trend	-3.041$^{(*)}$	demean and trend	-62.298	0.000

H0: all panels contain unit roots, Ha: some panels are stationary.
critical values for CIPS ($N = 200$,$T = 10$, Pesaran (2006, 2007)).
intercept : -2.28 (1%), -2.10 (5%), -2.01 (10%).
intercept + trend : -2.98 (1%), -2.75 (5%), -2.63 (10%).
(*): the test rejects the null hypothesis of unit roots at the 5% level.

D.2. Short run and long run direct, indirect and total effects

Pooling the N counties, we can re-write the DGNSP-CCE specification as

$$Y_t = \lambda W_N Y_t + \phi Y_{t-1} + \rho W_N Y_{t-1} + x_t\beta + W_N x_t \gamma + \Gamma f_t + u_t \ , \ t = 1, ..., T, \quad \text{(D.1)}$$

where $Y_t = \log R_t$, $x_t = [\log Q_t, \ \text{urban rate}_t, \log P_t]$. Then, we can write

$$\begin{aligned} Y_t &= Q^{-1}\left[x_t\beta + W_N x_t\gamma + \Gamma f_t + u_t\right] \\ &= \sum_{k=1}^{K} Q^{-1}\left[x_{k,t}\beta_k + W_N x_{k,t}\gamma_k\right] + Q^{-1}\left[\Gamma f_t + u_t\right] \end{aligned}$$

where $x_{k,t}$ is the kth variable of x_t and with

$$Q = \begin{pmatrix} B & 0 & 0 & \cdots & 0 & 0 \\ A & B & 0 & \cdots & 0 & 0 \\ 0 & A & B & \cdots & 0 & 0 \\ \cdots & \cdots & \cdots & \cdots & \cdots & \cdots \\ 0 & 0 & 0 & \cdots & A & B \end{pmatrix}, \ A = -\left(\phi I_N + \rho W_N\right) \text{ and } B = \left(I_N - \lambda W_N\right)$$

leading to (see Debarsy et al. (2012))

$$Q^{-1} = \begin{pmatrix} B^{-1} & 0 & 0 & \cdots & 0 & 0 \\ D_1 & B^{-1} & 0 & \cdots & 0 & 0 \\ D_2 & D_1 & B^{-1} & \cdots & 0 & 0 \\ \cdots & \cdots & \cdots & \cdots & \cdots & \cdots \\ D_{T-2} & D_{T-1} & D_{T-3} & \cdots & D_1 & B^{-1} \end{pmatrix} \text{ with } D_s = (-1)^s \left(B^{-1}A\right)^s B^{-1}$$

Then, the τ-period ahead (cumulative) impact arising from a permanent change at time t in $x_{k,t}$ is

$$\frac{\partial E\left[Y_{t+\tau}\right]}{\partial x'_{k,t}} = \sum_{s=0}^{\tau-1} D_s \left[I_N \beta_k + W_N \gamma_k\right]$$

and the impact multiplier (or short run effect) is

$$\frac{\partial E\left[Y_t\right]}{\partial x'_{k,t}} = B^{-1}\left[I_N \beta_k + W_N \gamma_k\right] = \left(I_N - \lambda W_N\right)^{-1}\left[I_N \beta_k + W_N \gamma_k\right]$$

Since these (impact and cumulative) multipliers are $(N \times N)$ matrices, the (impact or cumulative) direct effect is the $(N \times 1)$ vector of the diagonal elements of these matrices. The (impact or cumulative) indirect effect is the $(N \times 1)$ vector of the row sums of the non-diagonal elements of these matrices. And, the (impact or cumulative) total effect is the $(N \times 1)$ vector of the row sums of these matrices. The average direct, indirect and total effects are the averages of these $(N \times 1)$ vectors.

By considering the reduced form of the model (D.1)

$$\begin{aligned} Y_t &= \left(I_N - \lambda W_N\right)^{-1}\left(\phi + \rho W_N\right) + \left(I_N - \lambda W_N\right)^{-1}\left(x_t \beta + W_N x_t \gamma\right) \\ &\quad + \left(I_N - \lambda W_N\right)^{-1}\left(\Gamma f_t + u_t\right) \end{aligned}$$

the long run effect ($\tau \to \infty$) is given by (see Elhorst, 2021)

$$\frac{\partial E\left[Y_\infty\right]}{\partial x'_{k,t}} = \Big(\left(1-\phi\right) I_N - \left(\lambda + \rho\right) W_N\Big)^{-1}\left[I_N \beta_k + W_N \gamma_k\right]$$

References

Ahn, S.C., Horenstein, A.R., 2013. Eigenvalue ratio test for the number of factors. Econometrica 81, 1203–1227.

Cattell, R.B., 1966. The scree test for the number of factors. Multivariate Behavioral Research 1, 245–276.

Debarsy, N., Ertur, C., LeSage, J.P., 2012. Interpreting dynamic space–time panel data models. Statistical Methodology 9, 158–171.

Elhorst, J.P., 2021. The dynamic general nesting spatial econometric model for spatial panels with common factors: Further raising the bar. Review of Regional Research , 1–19.

Onatski, A., 2010. Determining the number of factors from empirical distribution of eigenvalues. The Review of Economics and Statistics 92, 1004–1016.

Pesaran, M.H., 2006. Estimation and inference in large heterogeneous panels with a multifactor error structure. Econometrica 74, 967–1012.

Pesaran, M.H., 2007. A simple panel unit root test in the presence of cross-section dependence. Journal of Applied Econometrics 22, 265–312.